Nanoscale Advances

ROYAL SOCIETY OF CHEMISTRY

REVIEW

View Article Online
View Journal | View Issue

Cite this: *Nanoscale Adv.*, 2025, **7**, 3914

Application of the synergism between eggshells and copper in nanotechnology

Priyanka Sharma,[a] Mainak Ganguly *[a] and Ankita Doi[b]

Eggshells, the non-edible part of an egg, have immense uses in nanotechnology. Copper being an inexpensive metal has versatile applications in nanotechnology. However, its susceptibility to oxidation limits its practical applications. Eggshells are an efficient candidate to synthesize cap copper nanoparticles and copper nanoclusters, which are used in various arenas (dye degradation, antibacterial activity, nitrophenol adsorption, copper adsorption, and sensing). Reports on the edible part of an egg for passivating copper nanoparticles are rare. Usually, chicken eggshells are mostly used in this regard. Moreover, eggshells can be used for the adsorption of ionic copper. Thus, the synergism between eggshells and copper is a very pivotal aspect. The use of biological waste in association with copper in various applications may open a new pathway towards the circular economy. This review article summarizes applications that evolved from copper–eggshell synergism.

Received 24th April 2025
Accepted 25th April 2025

DOI: 10.1039/d5na00400d

rsc.li/nanoscale-advances

1. Motivation

As a natural porous bioceramic, chicken eggshells are formed *via* the gradual accumulation of various layers around the albumen of the hen oviduct.[1] The eggshell is a well-organized structure with a polycrystalline organization throughout the calcified shell. Currently, the applications of eggs are the subject of extensive research.[2,3] Over the past several years, significant research has been conducted to develop goods that use eggshells as a value-added component.

Eggshells and their environmental applications have been the subject of numerous extensive studies that have been documented in the literature.[4–8] A review paper based on the biosynthesis of metallic nanoparticles using bacterial cell-free extract was published last year in the *Journal Nanoscale*.[9] Likewise, we would like to publish a paper based on the role of eggshells in passivating copper nanoparticles. Thus, we consider *Nanoscale Advances* a suitable journal for publishing this manuscript.

The change in the size of nanoparticles is related to a variety of physicochemical parameters associated with the particles.[10] In the visible region, for instance, copper nanoparticles are

[a]*Solar Energy Conversion and Nanomaterials Laboratory, Department of Chemistry, Manipal University Jaipur, Dehmi Kalan, Jaipur 303007, India. E-mail: mainak.ganguly@jaipur.manipal.edu*

[b]*Department of BioSciences, Manipal University Jaipur, Jaipur-Ajmer Express Highway, Dehmi Kalan, Jaipur, Rajasthan 303007, India*

Priyanka Sharma

Priyanka Sharma obtained her BSc and MSc degrees from Maharaja Brij University in India. She is now pursuing her PhD degree at Manipal University Jaipur, India, under the guidance of Dr Mainak Ganguly. Her area of interest is material science and environmental science.

Mainak Ganguly

Dr Mainak Ganguly received his PhD from the Indian Institute of Technology, Kharagpur, India in 2014. He had acted as a post-doctoral researcher up to 2019 in Furman University (USA) and McGill University (Canada). He is currently working as an Associate Professor in the Department of Chemistry, at Manipal University Jaipur (India). His research interests include nanoparticles, clusters, biophysical chemistry, environmental remediations, etc. He has published more than 75 papers and two book chapters.

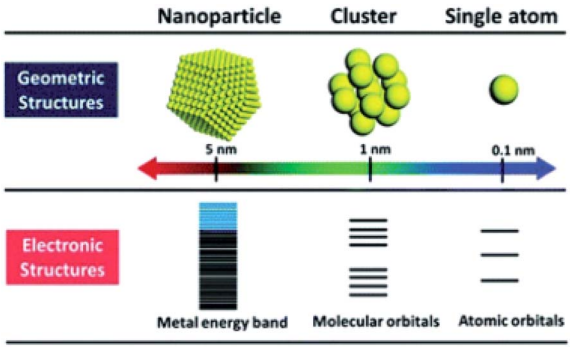

Fig. 1 Structure of nanoscale metal materials. This figure has been adapted/reproduced from ref. 18 with permission from *Nanoscale Adv.*, copyright 2021.

responsible for the formation of surface plasmon bands, whereas copper nanoclusters display fluorescence because of the d–d transition process. It is necessary to review these methods because the nanosensing involving copper nanoparticles and copper nanoclusters is relatively distinct from one another. However, eggshell-capped copper nanoparticles and copper nanoclusters have not been simultaneously reviewed to date. This is the first time that a comprehensive review of eggshell-capped copper nanoparticles and nanoclusters in nanotechnology with a circular economy has been thoroughly documented. This review article will be beneficial not only to material scientists but also to general readers as our capping agents come from kitchen trash bins.

2. Introduction

Particles that have at least one dimension within the range of 1–99 nanometers are referred to as nanometer-sized particles (NAPs).[11] Nanoparticles must possess a surface plasmon band to accomplish applications in sensing, imaging, and catalysis. The characteristic of this band is that it is defined by the collective oscillation of electrons on the surface of the nanoparticles, which results in a unique absorption peak in the spectrum that spans the ultraviolet and visible regions.[12]

Ankita Doi

Ankita Doi received her graduation from Alankar P.G. Mahavidyalaya (Jaipur, Rajasthan, India) and Postgraduate from Alankar P.G. Mahavidyalya (Jaipur, Rajasthan). Currently, she is pursuing a PhD from Manipal University, Jaipur under the supervision of Dr Mainak Ganguly. Her research area is nanoparticles.

The degree of interest in near-monodispersed particles, which are typically less than 10 nanometers (100 Å) in diameter, has experienced a significant increase over the past decade. On the other hand, nanoclusters are considered by some researchers to be NAPs smaller than two nanometers. When NACs lose their surface plasmon bands, which are distinguished by different energy levels, they lose their emissive properties. NACs are responsible for these features. As the missing connection between atoms and NAPs, NACs are suitably deemed the missing link between the two.[13–16]

Compared with other precious metals, copper is available in relatively large quantities and is relatively affordable. CuNACs, on the other hand, are less stable than other materials because of their high oxidation susceptibility, and their luminescence quantum yield is lower. Additional characteristics analogous to those of electrons at Fermi wavelengths are present in metal nanoclusters smaller than 2 nanometers.[17] These properties include molecular-similar and size-dependent ocular and fluorescent traits, intrinsic magnetism, strong chiral responses, and other related properties. When plasmonic atoms interact with an electromagnetic field, the collective fluctuations of the conduction band electrons, which are typical for plasmonic atoms, are no longer dominating. This is because the ultrasmall size regime, which divides the continuum of energy bands into different energy strata, results in the separation of energy bands into distinct energy strata. In the optical absorption spectra of discrete and quantized states, abundant molecular-like properties can be observed. In addition to being exceptionally stable naturally occurring compounds (NACs), noble metal clusters exhibit several features [Fig. 1].[18–24] The durability of atomically precise CuNACs, on the other hand, is a major worry because the metal is extremely susceptible to oxidation. Over the last several decades, the stability problem has been significantly addressed by the development of synthetic processes, the utilization of mild and inert settings, and the selection of appropriate ligands that possess unique structures and strong metal binding affinities. It is important to establish links between Cu based nanoparticles and waste eggshells.

The development of biodegradable polymers and composites based on these materials is experiencing a new trend. Although certain biodegradable polymers are available, such as cellulose, polylactic acid, polypropylene carbonate, poly(3-hydroxybutyrate-*co*-3-hydroxyvalerate), and others, these polymers do not possess adequate strength and thermal stability.[25] Additionally, most of them are more expensive than synthetic polymers such as polyethylene and polypropylene, which are examples of synthetic polymers. Some waste resources include tamarind nut powder, eggshell powder, wasted tea leaf powder, waste leather buff powder, and other waste materials.[26–28] During the manufacturing process of biocomposite, these waste products were utilized as fillers in conjunction with biodegradable matrix materials.[29–35] Some of them include egg shells, which are a sort of waste that is produced in enormous quantities all over the world and is related to poultry and kitchens. Egg shells are a type of waste. There are various environmental and health problems that can be caused by these eggshells if they are not disposed of properly.[36]

Table 1 Published review articles related to ES available in the literature

Papers	Focus
Mittal *et al.*[47]	The applications of ES and the ESM.
Baláž *et al.*[48]	Utilized eggshell waste for very diverse purposes, stressing the need to use a mechanochemical approach to broaden its applications
Iftikhar *et al.*[49]	The valorization pathways and methods for extraction of CaO and exploring the chemistry of eggshell
Kumar *et al.*[50]	Calcium phosphate (CaP) precursors from eggshells for improving the bone cement formulations. Eggshell CaP-based scaffolds in tissue engineering and regenerative medicine
Owuamanam *et al.*[51]	Recycled bio-calcium carbonate fillers (uncoated/unmodified) in polymer composites with a focus on tensile strength, flexural strength and impact toughness
Rosaiah *et al.*[52]	The evolution of eggshells' use in functional materials and their performance in various energy-related applications
Badamasi *et al.*[53]	The efficient photocatalytic removal of organic dyes from water and wastewater using ESWM-supported MO nanocomposites
This work	A thorough examination of the current state of research on eggshell-capped copper nanoparticles, focusing on the synthetic methods, characterization techniques, applications, challenges, and future perspectives

Eggshell powder (ESP) was used as a filler in the biodegradable films created for packaging purposes. These films were made using polylactic acid and polypropylene carbonate as matrices.[37–39] In addition, several researchers have discovered further applications for egg shells, a waste product of poultry that is consistently produced in large quantities. In a study conducted using this approach, ESP was applied to immobilize cadmium and lead in soil that was polluted.[40] These waste bird eggshells, which come from chickens, ducks, ostriches, and quails, are examples of natural biomaterials that are easily available.

According to estimates, more than 8 million tons of waste eggshells are produced annually worldwide. The eggshell is composed of roughly 94% $CaCO_3$, 1% $Ca_3(PO_4)_2$, 1% $MgCO_3$, and 4% organic components (mostly proteins).[41] $CaCO_3$, with functional groups like C=O and C–O, has a strong ability to grab and connect metal ions. The compound $CaCO_3$, which possesses functional groups such as C=O and C–O, binds and links metal ions with remarkable capacity. Three layers make up the construction of the eggshell: a thin mammillary inner layer that does not include any pores, a thick palisade middle layer that has numerous large pores, and a thin cuticle outer layer that does not contain any pores. Zhao *et al.*[42] developed a CuSe/$CaCO_3$ composite for calcium silicate boards using biowaste resources, in this case, rice husk and oyster shell. CuSe/$CaCO_3$-loaded calcium silicate boards reduced bacteria (*E. coli*, *S. aureus*) and fungus (*C. albicans*) growth. The appropriate loading quantities and processing conditions for antibacterial action and flexural strength were determined. They improved building materials with environmental care to produce healthy living environments.

The surface of the eggshell is composed of around 7000–17 000 funnel-shaped canals that are scattered unevenly, making it a perfect medium for the transmission of energy and mass. To recycle metal nanoparticles, waste eggshells, which are a good bio-template, may be recycled as a carrier that is both cost-effective and ecologically beneficial.[43,44] Natural processes can produce nanoparticles, and their presence may be found everywhere. Nanoparticle clusters, also known as nanoclusters, are a kind of nanoparticle that is sufficiently tiny to be less than 2 nanometers in size. To create various applications, a substantial amount of effort has been made to synthesize both nanoclusters and nanoparticles in the laboratory.[45]

In this investigation, a difficulty is the balancing of size and form, in addition to the stability concerns. Within the framework of this discussion, it is of utmost importance to ascertain the experimental circumstances and capping agents.[46]

This review provides a thorough examination of the current state of research on eggshell-capped copper nanoparticles. This review discusses the synthesis methods, characterization techniques, applications, challenges, and future perspectives [Table 1]. The goal is to highlight the potential of these nanoparticles and identify areas for further research.

3. Eggshell

Eggshells, which are primarily composed of calcium carbonate, are a biocompatible and eco-friendly material. They can act as a capping agent for nanoparticles, providing stabilization and preventing agglomeration.[54] Using eggshells not only offers a sustainable approach but also adds value to waste materials, aligning with the principles of green chemistry. The integration of eggshells into nanoparticle synthesis provides an innovative method to enhance the stability and functionality of copper nanoparticles. The egg comprises components such as the cuticle, eggshell membranes, calcified eggshells, and albumen, which surrounds the yolk, which is the center of the egg.[55–60]

Birds, particularly domestic chickens, have a well-defined mechanism for egg production, with detailed knowledge of each egg compartment's spatial and temporal control.[61,62] In chickens, each egg is shelled and then expelled (oviposition) at regular intervals, such as every 24 hours. Over ninety-six percent of an eggshell comprises calcium carbonate, one percent magnesium carbonate, one percent calcium phosphate, organic components (mostly proteins), and water. The applications ranged from developing improved materials for bone tissue healing (hydroxyapatite) to using them as adsorbents for metal ions [Fig. 2]. Recent research demonstrates that eggshell waste

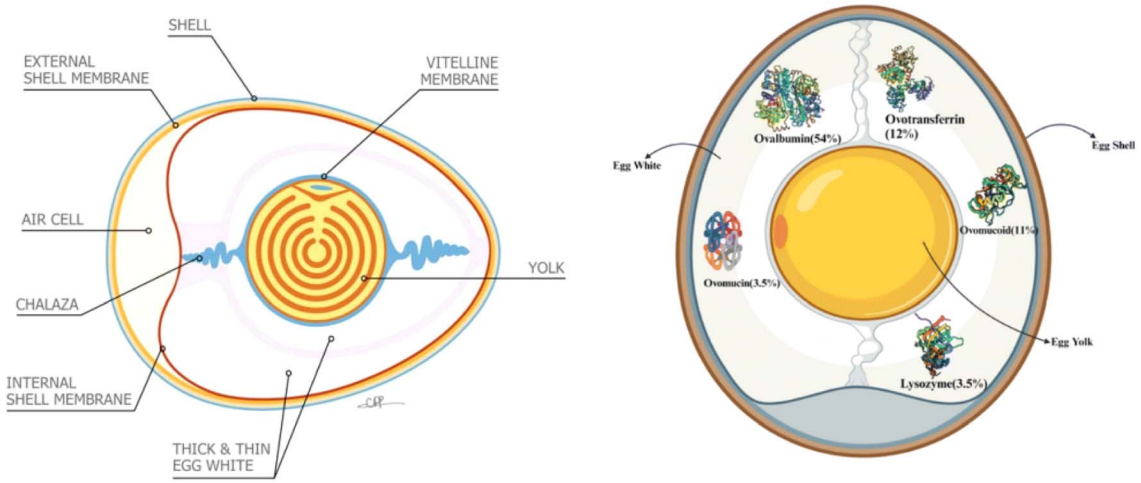

Fig. 2 Structure of an egg. This figure has been adapted/reproduced from ref. 63 with permission from *Frontiers in Bioscience*, copyright 2012, and from ref. 64 with permission from *Sustainable Food Technol.*, copyright 2024.

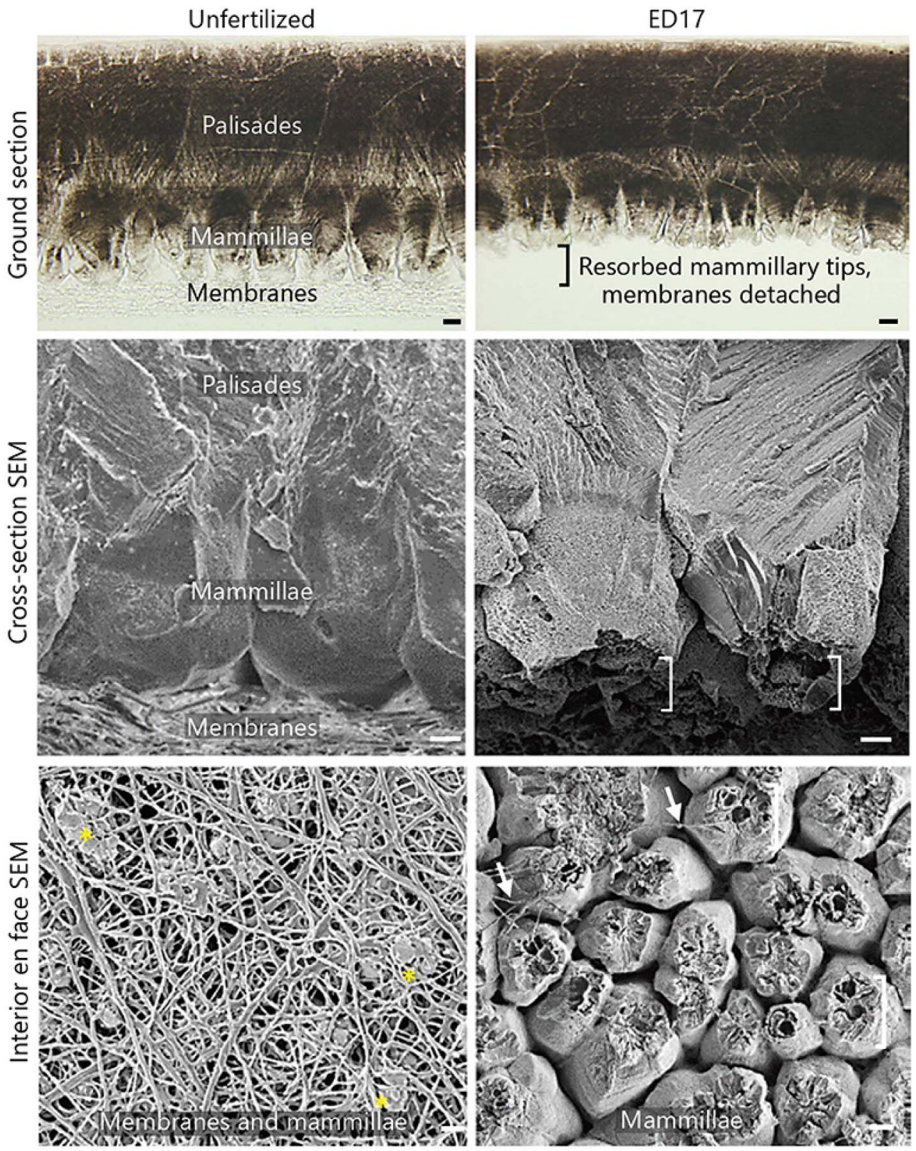

Fig. 3 Morphology of the ES/ESM of a fertilized and unfertilized egg. This figure has been adapted/reproduced from ref. 65 with permission from *Front. Bioeng. Biotechnol*, copyright 2021.

Table 2 S_{BET} and average particle size of ES powder and $CaCO_3$

	Sample	Surface area (m^2 g^{-1})	Average particle size (μm)
1	Eggshell	3.5421	3
2	Ballmilled eggshell	0.3265	35
3	$CaCO_3$	0.014	49
4	$CaCO_3$, US 1 h	0.02	47
5	$CaCO_3$, US 2 h	0.08	44
6	$CaCO_3$, US 3 h	0.1	41

can be used as an environmentally acceptable catalyst for nanoparticle detection in various processes.[63,64]

Eggshell provides a barrier against pathogens and is permeable to gas exchange because of its porosity. However, after fertilization, the eggshell begins to degrade as calcium is used to develop the chick embryo. Therefore, the mammillary layer's bottom part is dissolved, and the eggshell membrane detaches. Fig. 3 shows a comparison of the morphology of ES/ESM between fertilized and unfertilized eggs is provided.[65]

Higher S_{BET} values with smaller catalyst particles may enhance the reaction conversion. The particle size and nitrogen physisorption of pure $CaCO_3$ and natural eggshells were investigated. The surface area of the ball mill-treated eggshell was 0.0253 m^2 g^{-1} with an average particle size of 35 μm. In comparison, nano-eggshell powder (NESP) had 3.5421 m^2 g^{-1} and 3 μm, indicating a reduction in powder crystal size after ultrasonic irradiation. Poor surface area and greater particle size in pure $CaCO_3$ and its sonicated versions resulted in poor porosity [Table 2]. Since the specific surface area and catalyst particle size matched the catalytic activity, mesoporous sonicated eggshells with miniaturized crystals may catalyse the process better than ball-milled eggshell powder and $CaCO_3$.[66]

Eggshell collagen protein consists mostly of glycine, proline, and hydroxyproline. Proline forms an intermediate silver–amino acid combination with two hydroxyl groups. This rearrangement generates AgNPs and AgONPs [Fig. 4]. The nanocomposite eggshell powder (NCESP) lowered the strength of the two peaks at 1654 and 1481 cm^{-1}, indicating that the ESP protein component contributed to AgNP and AgONP synthesis.[67]

3.1 Eggshells have some salient properties to mention

(1) Composition: eggshells are mostly composed of calcium carbonate, which accounts for approximately 94–97% of eggshell content. Additionally, eggshells contain trace amounts of $MgCO_3$, $CaCO_3$, and organic proteins. The presence of these compounds contributes to the adsorptive properties of eggshells.[68]

(2) Surface area and porosity: the porous structure of eggshells provides a large surface area for adsorption. The micro- and mesopores in the eggshell matrix enhance the adsorption capacity by providing more active sites for pollutant binding.

(3) Functional groups: several different functional groups, including hydroxyl, carboxyl, and carbonate groups, are found on the eggshell surface. These functional groups play a crucial role in the adsorption process by interacting with pollutants through various mechanisms such as ion exchange, complexation, and hydrogen bonding.

4. Application of eggshells

Farming procedures generate several types of trash. To address the environmental issues caused by improper waste disposal, it is crucial to effectively utilize agricultural waste. Effective management of agricultural waste is critical for the health of humans, animals, and plants worldwide. Waste types and quantities vary by country. Effective management of agricultural waste is crucial for protecting the environment and health.[69–71] Waste should be recycled, repurposed, and converted into useful products. Effective waste management is crucial for sustainable development.

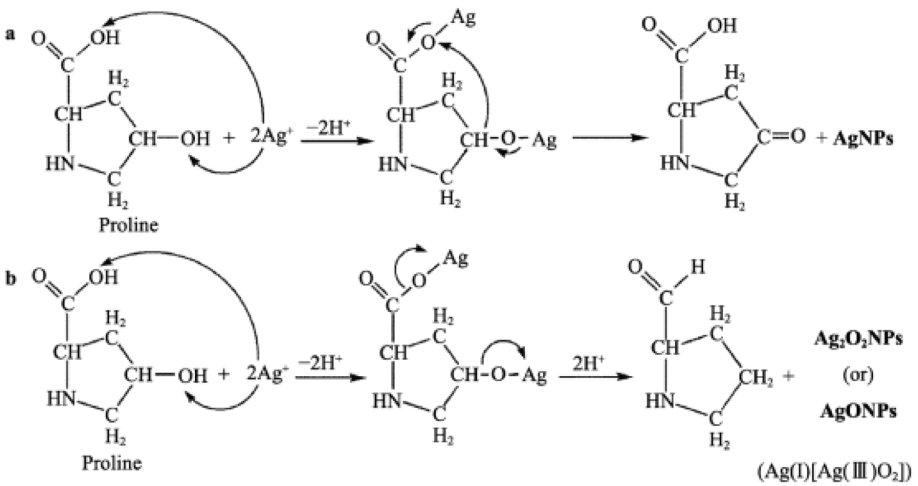

Fig. 4 Mechanism for the formation of (a) AgNPs and (b) Ag_2O_2NPs/AgONPs involving proline. This figure has been adapted/reproduced from ref. 67 with permission from the *Journal of Bioresources and Bioproducts,* copyright 2020.

The processing of food and the manufacturing of goods frequently result in the production of eggshells as a byproduct.[72] Eggs are frequently used in a broad variety of products, such as cakes, salad dressings, and fast food, resulting in substantial instances of waste and considerable costs associated with disposal worldwide. Approximately 250 000 tons of eggshell waste are produced in the world every single year. As of the current study, most of the eggshell trash is gathered on-site without being pre-treated. Because biodegradation produces a foul smell, waste management can be an unpleasant experience.[73]

Recent efforts have focused on transforming discarded eggshells into a commodity that may be put to beneficial use. As a bone replacement, as a starting material for calcium phosphate bioceramics such as hydroxyapatite (HAp), as a bone mineralization and growth agent, as a low-cost adsorbent for eliminating ionic contaminants from water, and as a biodiesel catalyst were the primary applications.[74–76]

There is not enough attention paid to the process of converting trash into valuable resources, even though there are many advantages associated with this process. In this context, eggshell waste offers suggestions to every egg processor, applicant, and customer. This was achieved by evaluating information on the technological potential of eggshell qualities.

4.1 Medical application of eggshells

Several active chemicals with potential medical use can be found in agricultural waste. Avian eggshells can be used to make HAp, an agricultural waste product. Calcium phosphate ceramics play a key role as biomaterials because of their osteophilic nature and ability to penetrate bone tissues.[77] Discarded eggshells are generally unused and untransformed. Eggshells contain calcium carbonate, which can be used to prepare HAp, a key component in bone and dental treatment. Using eggshells to make HAp reduces waste pollution and turns it into a valuable product for bone repair or replacement. It also has a minimal environmental impact.[78,79]

4.2 Application of eggshells in producing bio-diesel

CaO is a promising alkaline earth metal oxide with strong basicity and is ideal for bio-diesel synthesis. Calcinating mollusk, eggshell, and mussel shells can provide CaO, which can be used as a catalyst in biodiesel synthesis.[80] According to a previous study, discarded eggshell is primarily composed of calcium carbonate. Eggshell's pore structure and availability make it a suitable raw material for producing fine powder, which may lead to its use as a porous solid catalyst. Eggshell-derived solid base catalysts were created by calcination.[81–84]

4.3 Application of eggshells as fertilizer

Eggshells are responsible for the generation of a significant amount of biowaste each day worldwide. The smell of eggshells not only provides a breeding ground for flies and abrasiveness, but it also results in the loss of a great deal of material that may be helpful.[85] An application of eggshell waste discussed before is its potential use as a fertilizer for plants. This approach would be beneficial because it could help prevent the spread of plant blossom-end rot (BER) disease and the expenses associated with planting. It also helps plants absorb more nutrients. It will also be used to replace CIPCAL-500 in females as a calcium supplement tablet.[86]

4.4 Application of eggshells as adsorbents

Eggshells are a prospective low-cost and sustainable adsorbent for environmental remediation. Their ability to adsorb a broad variety of pollutants, such as heavy metals, dyes, organic contaminants, and anions, makes them a desirable material for water treatment applications. Eggshells are also a promising material for environmental remediation.[87–90]

Future research should focus on optimizing the pre-treatment processes, enhancing the regeneration capabilities, and exploring the adsorption mechanisms in greater detail to fully exploit the potential of eggshells as adsorbents. To prepare reusable materials from discarded eggshells, dry eggshells were crushed and calcined in a furnace at 800 °C for 2 hours. The natural eggshell has some potential to remove cadmium and chromium, but the elimination rate was poor, resulting in incomplete elimination even after 60 minutes.[91] Compared with cadmium and chromium, natural eggshells are more effective in removing Pb than calcined eggshells. The crystallites of eggshells in their crushed state have a surface structure that is uneven with pores that are around 200 nanometers in size. Similar photos have been reported for eggshells and pure calcite crystals. These photographs are comparable to those described.[92–94] The temperature was increased to 600 degrees Celsius, which resulted in the formation of a granular surface structure with a particle size of a few hundred nanometers [Fig. 5]. The surface exhibits a considerable degree of porosity. A densely packed structure was formed by the random assembly of individual micron-sized grains aggregated after being subjected to calcination at 900 degrees Celsius. The elemental dispersive analysis (EDS) study performed on these samples revealed that there were always representative peaks for calcium and oxygen, and this was the case for all the samples. The eggshells that had been crushed were found to contain traces of magnesium and carbon, consistent with what was anticipated.[95]

4.4.1 Adsorption of copper

4.4.1.1 Pure egg shells. Chou *et al.*[96] found that Cu^{2+} adsorption in an aquatic solution could be achieved using eggshell byproducts and treating calcined eggshells. Eggshell samples (eggshells (ESs), eggshell membrane (ESM), eggshells with the membrane (ESWM), and calcined eggshells (CSE)) were used to explore the impact of time on the adsorption of copper ions in aqueous solutions.

The adsorption rates of ES, ESWM, and ESM were 23.8%, 23.8%, and 19.1%, respectively, after one hour; after 48 hours, they were 66.7%, 53.9%, and 51.3%, respectively; and after twenty-four hours, they were 80.0%, 80.0%, and 73.3%, on average.[97] The rates also varied over time. At both 24 and 48 hours periods, the ES measurements showed no noticeable change. After twenty-four hours, a statistically significant difference was determined between ESM and ESWM.[98]

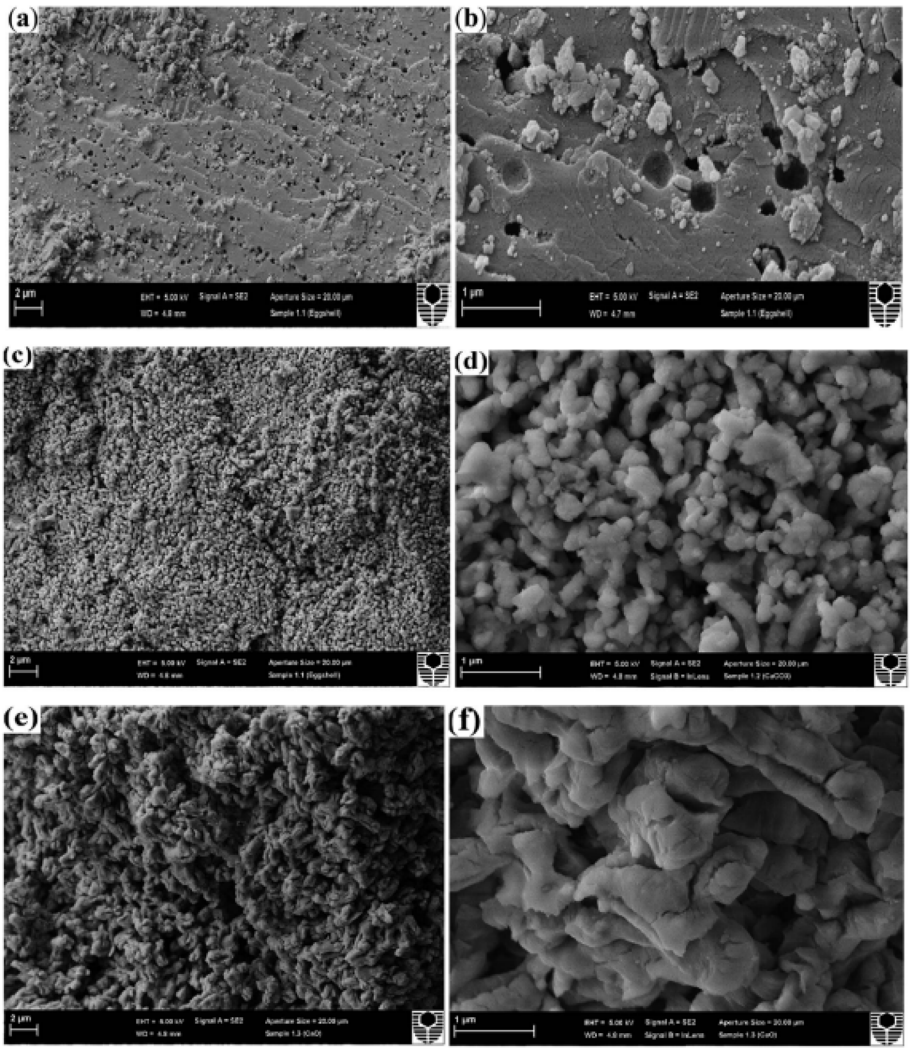

Fig. 5 SEM images of the eggshell (a and b) as-crushed and calcined at: (c and d) 600 and (e and f) 900 °C. This figure has been adapted/reproduced from ref. 95 with permission from *RSC Adv.*, copyright 2019.

The adsorption rates of CSE 1, CSE 2, and CSE 3 were all 93% when measured after an adsorption period of one hour. The maximum adsorption period was forty-eight hours, with adsorption rates of 94%, 97%, and 97%, respectively. When the adsorption period was reduced to just two hours, an adsorption rate of 92% was recorded for each of the three groups of CSEs. After one hour, the adsorption rates of CSE 4, CSE 5, and CSE 6 were 93%, 93%, and 100%, respectively.[99,100] After 48 hours, the maximum adsorption levels of 97.4%, 97.4%, and 100% were reached [Fig. 6 and 7].

The ES and ESWM adsorption rates at pH 5 were 95.2% and 90.5%, respectively, in a single factor, whereas the ESM adsorption rate at pH 5.9 was 73.3%. There was a significant difference between the two groups. To determine these outcomes, a reaction time of twenty-four hours, a metal concentration of twenty-five milligrams per liter, a dose of ten milligrams of adsorbent, and a temperature of twenty-five degrees Celsius were utilized.[100]

They discovered that every single group that included CSE-6 had a sufficient adsorption rate. After a response period of 20 minutes, the adsorption rate of CSE 2 achieved 99.3 percent. The response time ranged from 12 to 21.5 hours, higher than the adsorption rates of ES (93%), ESM (67.0%), and ESWM (76%).[101]

Markovic presented the bio-sorption (BS) of copper ions using raw eggshells as an adsorbent. The impact of the initial $[Cu^{2+}]$ demonstrated an increase in the BS capacity as the initial $[Cu^{2+}]$ rose, reaching a maximum at 800 mg dm^{-3}. The Langmuir isotherm was used to describe the BS process. The adsorption process occurred in a monolayer; however, there was a homogeneous distribution of active sites on the eggshell surface. In addition, the total number of adsorption sites was limited.[100,102–104]

When the pH level was 2, the BS capacity was around 10.82 mg g^{-1}. However, when the pH level was set to 5, the BS capacity exceeded double, reaching 21.62 mg g^{-1}. Because chicken eggshells are composed of approximately 95% calcium carbonate and 5% organic matter, the biosorption capacity of eggshells increases as the pH of the solution increases, allowing eggshells to absorb more water. The increase in the adsorbent mass from 0.2 to 1 g resulted in a greater number of accessible

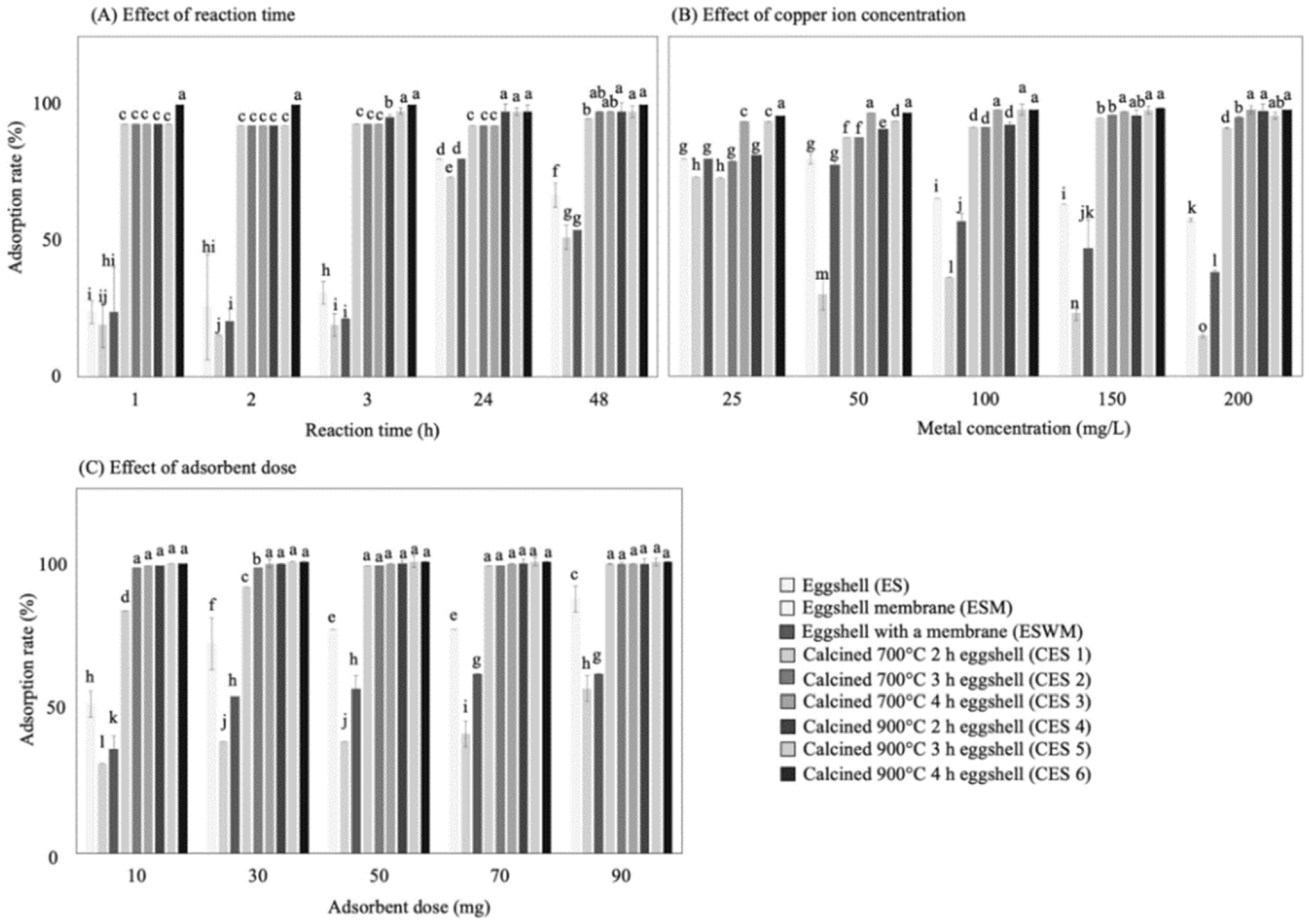

Fig. 6 Effect of the adsorption rates of differently treated eggshells with (A) reaction time, (B) Cu ion concentration, and (C) adsorbent dose. This figure has been adapted/reproduced from ref. 100 with permission from *Scientific Reports*, copyright 2020.

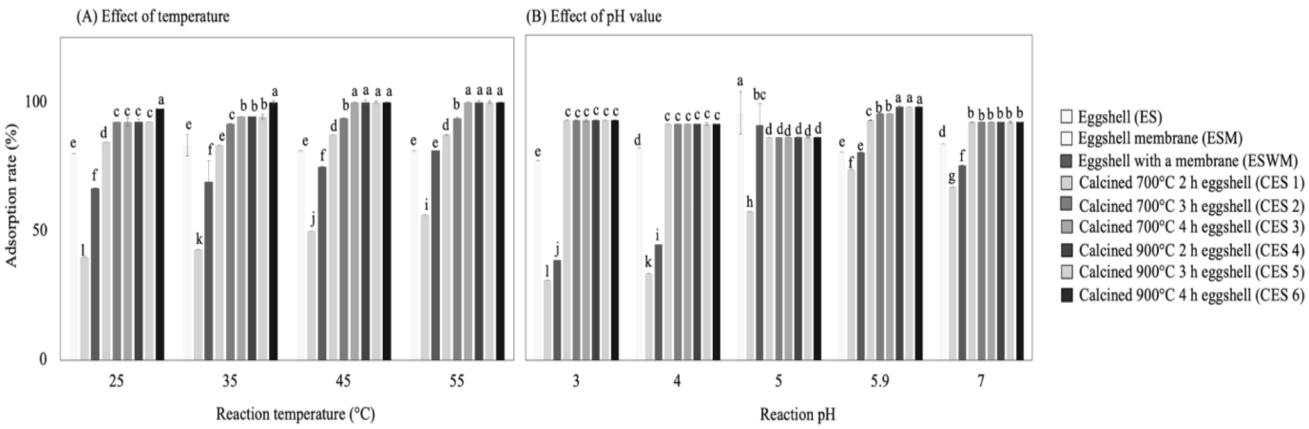

Fig. 7 Dependence of (A) temperature and (B) pH on adsorption behavior. This figure has been adapted/reproduced from ref. 100 with permission from *Scientific Reports*, copyright 2020.

active sites on the adsorbent structure, leading to an increase in the adsorption degree from 25% to 82%. This result can be attributed to the larger quantity of adsorbent [Fig. 6].

The surface structure of the untreated raw eggshell was both porous and dense. Copper ions were incorporated into the structure of the eggshell samples, resulting in a modest modification of the surface morphology. The surface became uneven, rough, and heterogeneous. The interaction of eggshells with Cu^{2+} ions led to the production of deposits on the surface of the adsorbent, resembling flake formation.

Zheng *et al.*[105] reported the adsorption of cadmium(II) and Cu(II) from aqueous solutions using eggshell waste-derived carbonate hydroxylapatite (CHAP). The [cadmium] and [copper] solutions ranged from 100 to 200 mg L^{-1}, and the pH was 5.0. Both Langmuir and Freundlich isotherms were detected. The CHAP used in this investigation had adsorption capabilities of 111.1 mg g^{-1} for Cd^{2+} and 142.86 mg g^{-1} for Cu^{2+}. There was no significant growth after this point, indicating the saturation of the CHAP active sites for metal ions. Approximately 90% of the metal ions were eliminated during the first 60 minutes, and no appreciable adsorption was obtained after 120 minutes. The contact time was 3 hours. The starting [cadmium(II)] and [copper(II)] were 80 and 60 mg L^{-1}, respectively, with a CHAP quantity of 0.5 g. Increasing the initial pH improved the metal ion removal efficiency. The mechanism of elimination was likely related to ion exchange. A large quantity of H^+ can shift the path of the reversible ion-exchange equilibrium at low pH. As the pH increased beyond 6, the removal efficiency decreased marginally, possibly due to the development of soluble hydroxy complexes.

According to Okure *et al.*,[106] the adsorption of copper(II), cadmium(II), and arsenic(III) ions on eggshells from aqueous solutions was observed under batch conditions at temperatures of 30, 40, 50, and 60 degrees Celsius, as well as at [copper(II)], [cadmium(II)], and [arsenic(III)] concentrations of 10, 20, 30, 60, and 80 milligrams per liter. As time passed and the [metal] ions in the solution increased, the partition coefficient of the ions that were transferred from the aqueous solution to the chicken eggshell also increased. However, the partition coefficient dropped with an increase in temperature, which was suggestive of physical adsorption on the eggshell.

At a temperature of thirty degrees Celsius, the fluctuation in the [metal ions] in solution after sorption and the concentration of adsorbed ions increased with time. Over time, the amount of metal ions adsorbed onto the eggshell surface increased. As time progressed, a greater proportion of the metal ions present in the bulk solution migrated through the boundary layer of the adsorbent and onto the active sites of the adsorbent. An increase in the kinetic energy of the hydrated metal ions might be responsible for the improved sorption of metal ions with increasing agitation duration. The improvement is due to a decrease in the boundary layer barrier to mass transfer in bulk solutions. A consistent decline in the removal efficiency of the adsorbent for the three metal ions was observed when the temperature was increased from 30 degrees Celsius to 60 degrees Celsius. The interaction between the eggshell surface and the metal ions in the solution was likely affected by temperature.[107]

Ofudje *et al.*[108] demonstrated that the waste generated from eggshell powder can be used as an inexpensive adsorbent for the removal of Cu^{2+} and reactive yellow 145 (RY 145) dye from an aqueous solution. SEM images of the eggshell before and after adsorption revealed approximately spherical particles agglomerating on the adsorbent surface. After pollutant adsorption, the open holes on the eggshell surface were no longer visible. The distributed adsorbate particles filled the unoccupied spots on the eggshell-derived calcium carbonate adsorbent (ESCCA) surface. In addition, the concentration of pollutants increased pollutant adsorption. The Redlich–Peterson[109] and Sips isotherms,[110] which combine Langmuir and Freundlich[111,112] models, accurately match the adsorption data. The Redlich–Peterson model yielded coefficients (R^2) of 0.998 and 0.986, while the Sips model yielded 0.995 and 0.987 for copper(II) ions and RY 145. The maximum adsorption of copper(II) ions and RY 145 by ESCCA reached equilibrium at 80 minutes of contact time at an initial pollutant concentration of 150 mg L^{-1}, with (84.20 mg g^{-1}) for Cu(II) ions and (68.70 mg g^{-1}) for RY 145 dye.

Although the percentage of RY 145 dye that was absorbed increased from 25.73% to 84.05%, the percentage of Cu(II) that was absorbed increased from 34.43% to 93.56% when the dose of the adsorbent was increased from 10 mg to 25 mg. When the amount of Cu(II) and RY 145 dye was increased beyond that threshold (25 mg), there was no discernible increase in the removal efficiency of either substance. The active, unoccupied receptors on the surface of the adsorbent became saturated.[113,114] The percentage of Cu(II) ions removed from the solution increased as the pH increased to 5.0, but the percentage of RY 145 dye removed decreased significantly. The highest possible absorption of 95.20% and 88.50% was achieved for copper(II) ions and RY 145 dye, respectively, when the pH of the solution was increased to 5.0 and 2.0, respectively.

According to Bashir *et al.*,[115] Cu^{2+} ions from synthetically stimulated wastewater are absorbed by eggshells (ES), spent tea leaves, and their biochar. Copper adsorption on the ES increased over time until saturation was reached at 150 minutes. The adsorption capacity and removal efficiency were both relatively low during the first 30 minutes of contact time; the contact time increased, and both capacity and efficiency showed a significant increase until they reached their maximum level of saturation at the end of 150 minutes. A decrease in pH (acidic) reduced the removal effectiveness, and the clearance effectiveness decreased when the pH exceeded 6 (basic). The presence of fewer adsorbates led to lower adsorption. The greatest reported adsorption capacity (AC) was 422.5 mg g^{-1}, achieving an 84.5% elimination rate.[116]

4.4.1.2 Eggshells passivated nanocomposite. A porous membrane adsorbent, referred to as amino-ESM(AEMS), was created by Chen *et al.*[117] The adsorbent was created by grafting amino groups onto the eggshell surface. The removal of copper ions from the aquatic solution perfectly illustrates the AC of the AEMS. The surface morphologies of the pristine and copper ion-loaded AEMS-27 exhibited a network-like structure of notable significance.

This structure was observed on the surface of the unaltered amino-AEMS-27; the AEMS-27 consisted of protein fibers and cavities that were strongly cross-linked. Several white items, resembling plates, were positioned on the surface of the AEMS-27. It was feasible to make out these individuals. The aggregation of copper ions adsorbed on the surface of AEMS-27 is a hypothesis.

When the dosage of the adsorbent was increased from 0.2 to 0.4 g L^{-1}, the absorption capacity of AEMS-27 fell by a substantial amount, decreasing from 86.3 to 55.1 mg g^{-1} within a very short length of time. As the amount of adsorbent

in the mixture increased, the AC of the AEMS-27 steadily decreased. A dosage of 0.4 g L^{-1} of the adsorbent was used because it was not only effective but also inexpensive. Although the concentration of both electrolytes increased from 0 to 2.5 mmol L^{-1}, the adsorption capacity of AEMS-27 decreased from 55.45 to 46.13 mg g^{-1} for sodium electrolyte and from 55.45 to 42.12 mg g^{-1} for calcium electrolyte, respectively. The concentrations of both electrolytes increased.[118] On the surface of AEMS-27, sodium and calcium ions might compete with copper ions for the same adsorption sites. This would harm the AC of AEMS-27 because it would eliminate copper ions from the surface.

The ecologically friendly method of producing calcium nanopowder, which consists of 26% β-tricalcium phosphate (β-TCP) and 74% hydroxyapatite (HA), was demonstrated by Kalbarczyk *et al.*[119] using hen eggshells (biowaste). The Cu^{2+} adsorption rate was rapid, and the adsorption equilibrium in the system was attained after 30 minutes had passed. After that period, the normal value of Cu^{2+} that had been adsorbed remained at 86 mg g^{-1}. The pseudo-first-order and pseudo-second-order kinetic approaches were utilized to obtain information on the adsorption kinetics.[120] The pseudo-first-order model had a correlation factor (R^2) that was equal to 0.718, which was a very low value. In the pH range of 3–4.5, the adsorption increased from 76.0 mg g^{-1} to its maximum value of 101.4 mg g^{-1}, with the pH range falling between 3 and 4.5. The negative trend was noticed throughout the process of the solution's acidity lowering from 4.5 to 6.0. When the pH level was high, the value differences in the measurement findings were caused by precipitating copper hydroxide. An increase in temperature does not result in a consistent pattern of changes in the adsorption capacity of the substance.[121,122] In a temperature of 25 degrees Celsius, the Cu^{2+} adsorption was equivalent to 97.1 mg g^{-1} of the adsorbent. The adsorption efficiency reached a value of 91.3 mg g^{-1} when the temperature was increased to 35 degrees Celsius. This was a little drop, but it was still within the standard deviation. In addition, the adsorption capacity increased to 111.6 mg g^{-1} because of an additional temperature shift to 45 degrees Celsius.

4.4.1.3 Chitosan-coated eggshell. Mohammadnezhad *et al.*[123] demonstrated the use of chitosan-coated eggshell particles (CST-ES) as a bioadsorbent for the removal of copper ions from aquatic media. Image analysis using FE-SEM revealed the presence of ES particles with a particle size range of 100–200 μm and possessing a crystalline structure with rough and uneven surfaces. ES membrane fibers were observed on the surface of the ES particles. CST was dispersed in 0.2 M $C_2H_2O_4$ solution and precipitated with 1 M NaOH solution. The FE-SEM images of the CSTs showed a porous structure. Copper ions were eradicated by CST-ES particles after 2 hours, whereas ES particles achieved 69.3% removal efficiency within 7 hours. The equilibrium AC (q_e) values of the ES and CST-ES particles were 13.9 ± 0.4 and 19.6 ± 0.6 mg g^{-1}, respectively. The varied surface adsorption locations affected the adsorption kinetics of the particles. ES particles remove Cu(II) ions *via* adsorption and precipitation, both of which involve interactions with the surface of $CaCO_3$. The adsorption of [Cu(II)] occurs at low pH *via* complexation with the carbonate group C=O bonds.[124,125] In the adsorption procedures, the medium pH was crucial. Changes in solution pH affect copper adsorption by particles in the pH range of 2–5 because chitosan dissolves below pH 2, and copper ions precipitate above pH 5. Reduced pH of the medium lowered copper adsorption capabilities for ES or CST-ES particles. The chitosan and immobilized chitosan exhibit a similar trend for adsorbing Cu(II).[126]

Cao *et al.*[127] used waste eggshell membranes to adsorb Cu^{2+} in wastewater, converting them into copper(II)–copper(I)/biochar through speedy pyrolysis. The benefits of ES membranes and copper(II)–copper(I) are combined in this system. These advantages include excellent electrical conductivity, a high electrochemically active surface area, distinctive three-dimensional porous network features, and rapid charge transfer. The Randles circuit was used to fit the acquired impedance data. The value of the Randles circuit was determined based on the dielectric and insulating characteristics of the electrode–electrolyte interface. The redox process of $[Fe(CN)_6]^{3-/4-}$ produced a huge semicircle on the naked GCE electrode. However, the diameter of the semicircle on the Cu^{2+}–Cu^{+}/biochar modified GCE electrode was significantly lower. Cu^{2+}–Cu^{+}/biochar composite materials showed significantly lower electrical and mass transport resistances compared to bare GCE. Cyclic voltammetry was used to compare calcined pure-biochar/GCE to Cu^{2+}–Cu^{+}/biochar/GCE in a 5 mM $[Fe(CN)_6]^{3-/4-}$ solution at 50 mV s^{-1}. The Cu^{2+}–Cu^{+} resulted in faster electron transport between the electrode surface and the analyte. The current values of various reaction systems were measured in the presence of 0.2 M phosphate buffer (pH 7.0) at a scan rate of 50 mV s^{-1}. In the absence of nitrite, the electrode remained neutral, but the presence of the nitrite group resulted in a peak-type response, indicating oxidation reactions. Cu^{2+}–Cu^{+}/biochar composite resulted in a significantly higher oxidation current compared to the absence of the composite. This result is attributed to Cu^{2+}–Cu^{+} catalysis of nitrite [Fig. 8].

According to FE-SEM, the ESM has a visible vertical and horizontal alternating 3D network structure containing collagen and glycoproteins. The natural 3D network structure of ESM with several functional groups, such as amino and carboxyl groups, provides a platform for loading metal ions or nanoparticles. The porous, three-dimensional structure of copper(II)–copper(I)/biochar is fully coated with metal ions. When the pH range was 5.0–5.5 on the copper(II)–copper(I)/biochar/GCE electrode, the peak oxidation current increased with increasing pH. While increasing pH (5.5–7.0), the oxidation peak current dropped. Using the cyclic voltammetry technique, the impact of the scanning rate on the peak current of nitrite ion oxidation was examined to understand the mechanism of electrode reaction. Cyclic voltammetry study of copper(II)–copper(I)/biochar/glassy carbon electrode in 0.5 mM nitrite, PBS (pH 5.5), at various scan rates. The oxidation peak potential (E_p) changed positively with scanning rate, indicating the irreversible nature of the nitrite oxidation process [Fig. 8].

4.4.1.4 DFT theory for the adsorption of copper. Ayodele *et al.*[128] investigated the adsorption of copper and nickel ions in simulated and industrial wastewater using eggshell-derived

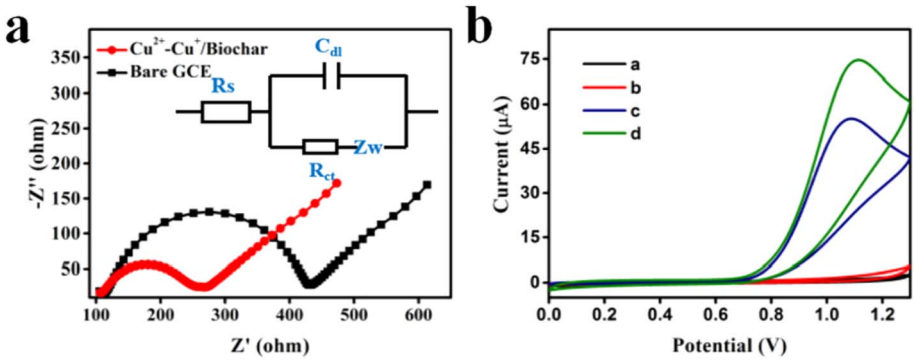

Fig. 8 (a) Nyquist plots; (b) cyclic voltammetric response of GCE and Cu^{2+}–Cu^{+}/biochar/GCE without (a and b) and with (c and d) of 1 mM sodium nitrite in pH-7 phosphate buffer at 50 mV s^{-1}. This figure has been adapted/reproduced from ref. 127 with permission from *Science of the Total Environment*, copyright 2020.

hydroxyapatite (HAp). The pH of a solution directly affects the quantity of adsorbed metal ions.[129] The (001) hydroxyapatite surface was modeled as a 2 × 2 slab with water molecules adsorbed. The $[Cu(OH)_2(H_2O)_4]$ and $[Ni(OH)_2(H_2O)_4]$ complexes were used as references for the surface adsorptive behavior. The Ca(II) and P adsorption sites were assessed. The complexes are in the bridge, three-fold, and on top of the adsorption site [Fig. 9]. The pseudo-second order and the Freundlich models accurately captured the adsorption kinetics and isotherms. The scanning electron micrograph shows a compact and coarse accumulation of particles on the surface, with a dispersion of tiny particles and big agglomerates.[130] The TEM picture shows dense, submicrometric HAp particles forming an interconnected macroporous network. Cu ion removal increased with resident time, peaking at 120 and 180 minutes at 100 and 200 mg L^{-1} values. The quick absorption of the metal ions was caused by the presence of more active sites early in the adsorption process.[131] However, as the amount of time that metal ions spent occupying the active sites increased, fewer active sites were accessible, which led to the adsorption of the metal ions on the surface of HAp progressing slowly. The adsorption process was aided by the longer contact time, which provided a longer residence time for metal binding. The adsorption sites for Ca(II) and P were examined and analyzed [Fig. 9]. The complexes are in the bridge, threefold, and on top of the adsorption sites. It is essential to use neutral complexes to ensure that the calculations are consistent. The OH acted as a bridge between Ni (or Cu) and the adsorption sites.[132]

4.4.2 Copper passivated eggshell nanocomposite as adsorbents. A hydrothermal metal oxide-assisted process was used to produce copper–calcium (CuCa) HSD (hydroxy double salts) materials.[133–135] Han *et al.*[136] focused on bio-based calcium oxide from waste eggshells (duck & quail eggshells) at different temperatures. The shells were then used as precursors for the synthesis of copper–calcium-HSD materials.

Eggshells-derived HSD was used to investigate the effectiveness of CuCa-HSD materials in removing methyl orange (MO)

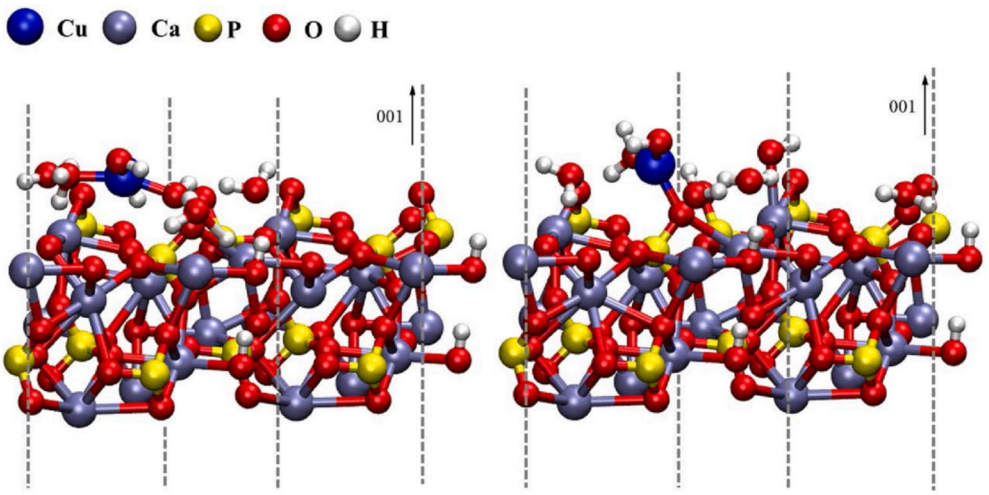

Fig. 9 Perspective view of the Cu(II) adsorbed on the (001) HAp surface. This figure has been adapted/reproduced from ref. 128 with permission from *Environmental Nanotechnology, Monitoring & Management*, copyright 2021.

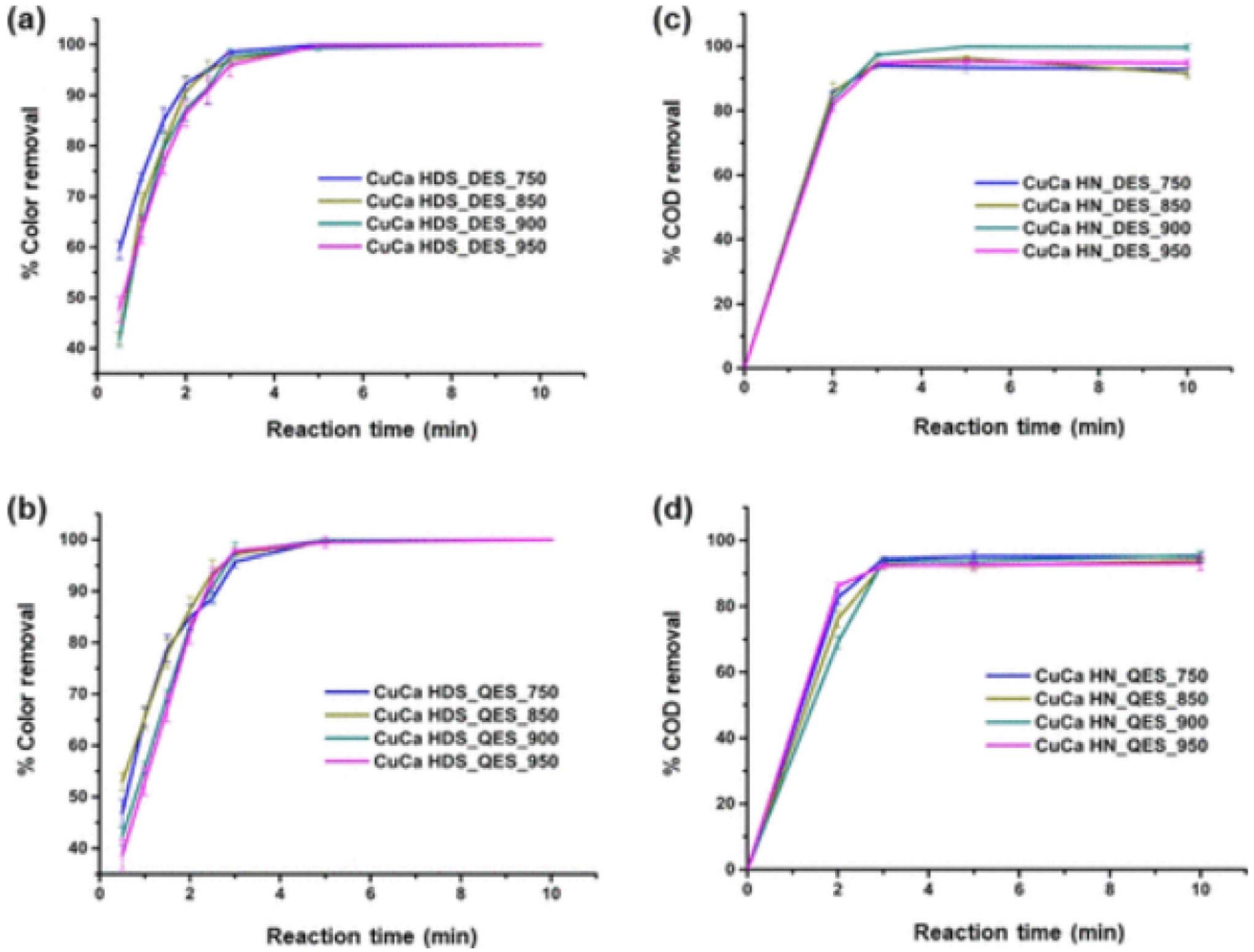

Fig. 10 Elimination efficiencies with time of MO(aq) in the presence of CuCa HSD from calcined DES (a) and QES (b) and % COD elimination efficiency with time employing the CuCa HSD from calcined DES (c) and QES (d). This figure has been adapted/reproduced from ref. 136 with permission from *ACS Omega*. Copyright 2023.

from aquatic solutions and the rates and efficiencies of MO removal.

The successful completion of the dye removal procedures was contingent on the structural integrity of the HSD materials and radical probing technologies. The temperatures for processing ESs and evaluating any changes in the activity of copper–calcium HSD synthesized from calcined ESs from different sources were the goals of this study. The effects of various calcination times on the effectiveness of copper–calcium HSD in methyl orange removal were observed. After only 2 and 5 minutes, respectively, the activity of copper–calcium HSD materials in decolorizing methyl orange under ambient circumstances and rapid color removal resulted in dye elimination efficiencies of more than 83 and 99% [Fig. 10]. After 5 minutes of MO removal in the presence of eggshell-derived CuCa HDS materials, COD was removed with greater than 90% efficiency. Thus, eggshell-derived CuCa HDS materials can purify highly contaminated waters (COD = 561 mg O_2 per L for 500 ppm MO).

Eggshell-derived with spent CuCa HSD displayed significant methyl orange elimination efficiency in the 1–2 cycles, but the efficiency decreased in the third cycle. Changes in the structure of HSD were brought about because of the intercalation activities that took place among methyl orange molecules and the nitrate anions in HSD.[137] The exchange between nitrate & methyl orange, and additional diffraction peaks at $2\theta = 4.4°$ were observed in the materials spent on HSD compounds.[138] This corresponds to a new *d*-spacing of 19.6 Å, which was a substantial increase in comparison to the brucite-like layer thickness of typical HSD materials, which was 4.8 Å.

4.4.2.1 Critical description. Studies have demonstrated the ability of eggshell-derived materials to adsorb heavy metals and dyes from aqueous solutions, making them a cost-effective water treatment option. Calcined eggshells (CSE) exhibited high Cu^{2+} adsorption rates and were responsive to pH, contact duration, and calcination procedure. Cd^{2+} and Cu^{2+} adsorption capabilities were high with carbonate hydroxylapatite (CHAP), but Okure *et al.*[106] found that temperature and metal ion concentration

affected efficiency. The eggshell powder successfully eliminated Cu^{2+} and reactive yellow 145 dye, aligning with Redlich–Peterson and Sips isotherms. The effectiveness of eggshells and biochar in adsorbing Cu^{2+} from wastewater, regulated by pH, was also studied. The porous membrane adsorbent (AEMS) significantly improved copper ion adsorption due to its protein fiber and cavity structure; however, larger doses lowered the performance due to ion competition. An eco-friendly approach was used to create calcium nanopowder from eggshells, attaining fast Cu^{2+} adsorption equilibrium; the performance varies by pH and temperature. The porous structure of the chitosan-coated eggshells increased the adsorption efficiency, achieving optimal performance in the specified pH ranges. Waste eggshell calcium oxide produced copper–calcium HSD materials with good methyl orange elimination efficiency, but cycles were reduced due to structural changes. This study highlighted the significance of material structure, pH management, and ambient variables in enhancing adsorption performance.

4.5 Passivation of copper nanoparticles

4.5.1 Choice of eggshells passivated copper nanoparticles. Nanotechnology is a new discipline of research that involves changing matter at the atomic or molecular level.[139] Nanotechnology is used to create tiny materials. This is a branch of research that studies the manipulation of atoms and molecules. One dimension of a nanoparticle (NAP) has a length that can range from one to one thousand nanometers, while its width can range from one to one hundred nanometers. The reduction method used and the environment surrounding the NAPs both play a role in determining their size.[140] The use of nanoparticles (NAPs) can be found in a wide range of biomedical and pharmaceutical applications, such as diagnostics, biomarkers, bioimaging, cosmetics, antibacterial, anticancer, immunology, cardiology, genetic engineering, drug delivery for cancer and other infectious diseases, bioremediation (environmental applications), water treatment, and energy production. The necessity for the biological synthesis of metal nanoparticles such as gold, copper, and others has significantly expanded in recent years. These nanoparticles have demonstrated impressive potential in terms of enhancing living standards.[141–144] Zhang *et al.*[145] demonstrated the impact of ES and metal ions on diabetic wound healing using a triboelectric nanogenerator (TENG). ES@$CuFe_2O_4$ nanocomposites (NCs) with a distinct structure and inherent antibacterial characteristics were synthesized. The nanocomposites were immersed in an oxidized starch hydrogel to form a multifunctional composite gel. A multifunctional composite gel was then created by embedding the as-prepared nanocomposites in an oxidized starch hydrogel. The gel was then combined to create a wearable ionic triboelectric nanogenerator (iTENG) patch using polydimethylsiloxane (PDMS). The "cocktail effect" on damaged tissue was caused by the tissue's ability to transform mechanical energy from human body motion to electric energy and release metal ions (Fe^{2+}/Ca^{2+}/Cu^{2+}). These effects could accelerate wound healing in diabetic mice by reducing inflammation, increasing angiogenesis, and depositing collagen.

Copper is required for metabolic activities in humans and animals. Although necessary for connective tissue crosslinking and iron and lipid metabolism, excessive exposure levels can cause toxicity. Copper can occur naturally in the environment as metallic (copper (0)), ionic (copper(I) or copper(II)), or manufactured CuNAPs.[146] These cupric forms cause varied levels of toxicity in living beings. Copper is found in the environment from various sources, including natural ores found in the crust of the earth and pollution from industrial processes. Copper is a versatile material that can be used for various purposes because of its distinctive physical and chemical characteristics. The physical characteristics of copper include a low rate of corrosion, high thermal and electrical conductivity, and easy malleability. Copper is referred to as "inert" because metal can only dissolve in acid when an oxidizing agent is present. Nevertheless, ionic copper can bind to various organic compounds, disrupting normal processes.[147]

Copper nanoparticles are used as additives in greases, polymers, and inks. CuNAPs, with their tiny size and capacity to release ions under acidic circumstances, have antibacterial capabilities and can be used as an addition in typical wastewater treatment. The qualities that make them useful for certain uses also have an impact on their toxicity potential.[148–150] Understanding toxicological mechanisms relies heavily on the physicochemical features of nanoparticle systems. Size, shape, crystallinity, aggregation, and surface coating are all examples of properties measured for particles. Ionic copper is less harmful to plants, aquatic species, rodents, and cell cultures than copper nanoparticles, which include zero-valent copper and copper(I) oxide (CuO). Copper nanoparticles are more cytotoxic than inorganic copper.[151]

4.5.2 Synthesis of copper nanoparticles *via* eggshell. The synthesis of eggshell-capped copper oxide nanoparticles is an eco-friendly process that uses eggshells as a natural capping agent. Clean, dried, and finely ground eggshells are mixed with a copper salt solution, typically copper(II) sulfate in water. As copper ions interact with the functional groups on the eggshell particles, a reducing agent like sodium hydroxide is added to form copper oxide nanoparticles. The eggshell components stabilize the nanoparticles, preventing clumping. After heating to promote crystallization, the nanoparticles are separated, washed, and dried. This method is valued for its simplicity, cost-effectiveness, and adherence to green chemistry principles.[152]

4.5.3 Application

4.5.3.1 Eggshell–Cu nanoparticles for dye degradation. A biotemplate approach was used by Wu *et al.*[153] to construct ES membranes (ESM)/cuprous oxide biomass catalysts using biological eggshell membranes. The equally loaded nanoparticles were woven together to form a network structure that was interlaced throughout the biomass catalysts. A significant degree of photocatalytic activity (k_{app} = 0.0392 min^{-1}) was observed in these biomass composites for methylene blue. Eggshell membranes were used as a sacrificial agent throughout the catalytic process. A considerable reduction in the rate, photogenerated electrons was observed. The amount of adsorbent used was 0.025 grams, and the amount of dye present was

30 milligrams per liter. The photodegradation rate reached over 97% in just one hour.

Xu *et al.*[154] synthesized CuO/eggshells using a simple method and used them as peroxymonosulfate (PSM) activators to remove reactive blue 19 (BR19). The CuO/eggshells achieved nearly 100% BR19 removal efficiency under optimal conditions (20 mg per L BR19, 0.2 g per L CuO/eggshells, 0.36 mM PSM, pH 7) within 20 minutes. The eggshell surface was rough with irregular pores, whereas pure CuO nanoparticles had a rod-like, uneven surface. The CuO/eggshells' morphology differed significantly, with CuO nanoparticles fully coating the eggshell surface. Lattice fringes corresponding to CuO and calcium sulfate were identified, but $CaCO_3$ spacings were not observed, likely due to $CaCO_3$ being covered by $CaSO_4$. Copper oxide/eggshell catalysts were easily produced and used to activate peroxymonosulfate (PSM). The target dye for evaluating the catalytic efficacy of copper oxide/eggshells was reactive blue 19 (BR19). PSM alone or copper oxide/eggshells alone had a minor effect on BR19 elimination, implying that PSM self-oxidation and copper oxide/eggshells self-adsorption could be ignored.[155] The ESs and PSM system demonstrated little BR19 elimination, showing that the ESs could not act as a catalyst to activate PSM. The copper oxide/eggshells and PSM methods showed considerable improvement, removing 99.72% of RB19 after 20 minutes. The copper oxide and PSM systems could degrade 99.05% of BR19 in 20 minutes; however, they were unsuitable as catalysts due to the rapid aggregation of CuO nanoparticles.[156] CuO used much more Cu than copper oxide/eggshells at the same catalyst dosage. The eggshell proved useful in inhibiting CuO nanoparticle agglomeration and promoting their dispersion. Copper oxide and eggshells exhibited synergistic effects to achieve great catalytic performance. When the catalyst dosage was increased from 0.025–0.1 g L^{-1}, the BR19 removal rate increased from 26.48% to 99.72%.

Gao *et al.*[157] reported the synthesis of a composite of eggshell-supported copper-doped FeOx NPs (CuFeOx/eggshells) using a co-precipitation technique. The catalytic performance of the CuFeOx/eggshells and peroxymonosulfate (PSM) system for carbamazepine (CZB) removal and the influence of the operating parameters and water matrices on CZB elimination are also presented. Reactive Oxygen Species (ROSs) were responsible for CZB oxidation and potential CZB break-down. Furthermore, several reaction mechanisms and degradation pathways were observed. The formation of CZB solution toxicity was also evaluated. The incorporation of CuFeOx/eggshells into PAN membranes increases the stability and minimizes metal releases.

Preda *et al.*[158] presented the characterization of biomorphic 3D-fibrous networks built on zinc oxide, copper oxide, and composite nanostructures consisting of zinc oxide and copper oxide. ESM is a bio-template consisting of two different kinds of metal salts, namely acetate and nitrate, as preparatory substances. The photocatalytic capabilities of the biomorphic metal oxide networks were assessed by evaluating the decrease in MB absorption intensity at its peak at ~664 nm. After 6 hours of irradiation, MB removal yielded ~67% for zinc oxide and ~50% for copper oxide networks, with the latter being equivalent to zinc oxide–copper oxide complex. A correlation between charge separation and composite networks with the maximum efficiency. Compared with composites with a lesser quantity of copper oxide (99.5 : 0.5 wt ratio) and a broader band gap (2.9 eV), zinc oxide–copper oxide complex fibers made with a higher amount of copper oxide (50 : 50 wt ratio) had a narrower band gap (1.94 eV) and a poorer photocatalytic activity.[159–163]

The synthesis of copper/ESs, iron oxide/ESs, and copper/iron oxide/ESs nanocomposites was accomplished by Nasrollahzadeh *et al.*[164] *via* an environmentally friendly and cost-effective approach that utilized an aqueous extract of the leaves of *Orchis mascula* L.[165–168] without any other additives. The surface roughness was altered in the presence of CuNPs. The copper nanoparticles were immobilized on the support surface, and a successful coupling of copper nanoparticles with the eggshell was achieved.

The copper nanoparticles had a restricted size distribution. The TEM micrographs demonstrated that the Cu NAPs had a spherical shape and an average diameter of around 5 nanometers. The average Fe_3O_4 NAP size was less than 22 nm. The porous nature of eggshell powder particles increases the contact area and facilitates Fe_3O_4 and copper loading. The Fe incorporation in the Fe_3O_4/eggshell nanocomposite was 24.69 wt%. TEM pictures of Fe_3O_4/eggshell nanocomposite. The Fe_3O_4 NAPs were very tiny, measuring <8 nm. TEM pictures show that the produced nanoparticles are mostly spherical and range in size from 5 to 15 nm.

The degradation of tetracycline hydrochloride (TCH) was accomplished using an ESs–CuS composite catalyst, which was effectively synthesized straightforwardly and used in conjunction with persulfate. According to Gao *et al.*,[169] the coated CuS had a structure similar to that of a sheet and was dispersed equally throughout the surface of the eggshell. Agglomeration enhances the performance of the catalyst. The enhanced catalytic effect compared to pure CuS was due to the production of a series of active species, including sulfate radicals (SO_4^-), hydroxyl radicals (OH), and carbonate radicals (CO_3^-), as confirmed by electron spin resonance (ESR) and free radical capturing. TCH remained stable at room temperature, with no obvious deterioration after 45 minutes. In the catalytic system, the strong oxidant-PS destroyed some of the TCH at room temperature, slightly increased sulfate radicals and moderate degradation (3.5%). The degradation rate of TCH by ES–CuS composites was limited to 9.2%, mostly due to their adsorption capability. Combining ES–CuS and PS efficiently degraded TCH, achieving a 93% degradation rate in 40 min. Conversely, the ES & persulfate and CuS & persulfate systems showed deterioration rates of only 28% and 62%, respectively. The modest deterioration of the ES & persulfate system might be due to the production of a tiny quantity of CO_3^- during catalysis.

4.5.3.2 Eggshell–Cu nanoparticles for nitrophenol degradation. Sajadi *et al.*[170] used a copper oxide/eggshell nanocomposite with pomegranate dried peel extract as an adsorbent nanocatalyst to effectively remove aromatic chemicals from crude oil samples. It was used for the reduction of 4-nitrophenol (4-NP) to 4-aminophenol at ambient temperature. Dried powdered ESs

and copper oxide nanoparticles were combined with distillate water under reflux conditions for 24 hours to progressively coat the CuO NPs on the eggshell to generate the CuO/eggshell nanocomposite. The addition of sodium borohydride to the 4-nitrophenol solution resulted in the formation of 4-nitrophenolate ions, as indicated by the emergence of an unchanged absorption peak at 400 nm without the presence of copper oxide or the ESs nanocomposite. When the catalyst was added to the mixture, a 4-aminophenol (4-AP) formed, and a new signal appeared at 297 nm.

CuO–ZnO (ZC) nanocomposites were developed utilizing bio-templated bio-waste-eggshell membranes (EMS) by He *et al.*[171] ZC–ESM nanocomposites retain the original structure of EMS with interlaced networks covered with tiny inorganic nanoparticles. After calcination, new samples form a rougher network structure with irregular nanoparticles. The average size of the synthesized nanomaterials follows the order copper oxide–EMS > zinc oxide–EMS > ZC–ESM, with CZ–EMS being the smallest. CZ–ESM nanocomposites have interparticular macroporosity but are still basically non-porous. They have low specific surface areas (<15 m2 g^{-1}) and pore volumes (usually 0.01 to 0.02 mL g^{-1}). The Brunauer–Emmett–Teller (BET) average pore size measures interparticular porosity, not real porosity [Fig. 11].

The high-resolution morphology of ZC–EMS nanocomposites showed well-dispersed particles with an average size of 100. The adjacent fringes had inter-planar *d*-spacings of 0.2778, 0.2069, 0.2414, and 0.2597 nm, corresponding to the lattice planes of monoclonal copper oxide and hexagonal zinc oxide, respectively. The ZC–EMS was a heterostructural nanocomposite. A study compared Congo red sorption characteristics in pure EMS, copper oxide–EMS, zinc oxide–EMS, and ZC–EMS nanocomposites. Copper oxide–EMS, copper oxide–EMS, and ZC–EMS nanocomposites exhibited considerably better sorption characteristics compared to EMS. In addition, ZC–EMS nanocomposites exhibited enhanced absorption. Dye molecules bind to ZC–EMS nanocomposites *via* electrostatic interactions and then enter the interparticular pores. As more molecules enter the pores, diffusion resistance rises, reducing the sorption rate. When the dye concentration decreases, the sorption slows until dynamic equilibrium occurs. When $NaBH_4$ was added without a catalyst, a 4-nitrophenol absorption peak was observed at 400 nm. With the addition of ZC–EMS, absorption gradually decreased after 12 minutes. 4-Aminophenol creation was confirmed by two additional bands at 300 and 230 nm. A catalytic effect comparison was conducted between different nanomaterials. Compared to their components, ZC–EMS nanocomposites exhibit optimal performance [Fig. 11].

The synthesis of copper oxide/zinc oxide/eggshell (CuO/ZnO/ES) nanocomposites from discarded eggshells was achieved using a deposition–calcination technique. Copper oxide and zinc oxide nanoparticles, ranging from 50 to 100 nanometers in diameter, were evenly dispersed on the eggshell surface. The resulting nanocomposites exhibit enhanced catalytic and photocatalytic reduction of 4-nitrophenol to 4-aminophenol in the presence of $NaBH_4$. The pure eggshells had a rough surface with irregular holes and pits measuring 100 to 400 nanometers. The nanocomposites showed significant morphological changes, with the surface densely coated with nanoparticles. ZnO/ES had a denser nanoparticle distribution than CuO/ES, and the combined CuO/ZnO/ES had larger nanoparticles due to the accumulation of copper oxide and zinc oxide.

At room temperature, the catalytic reduction of 4-nitrophenol (4-NP) to 4-aminophenol (4-AP) using sodium borohydride ($NaBH_4$) demonstrated the potential of nanocomposites for wastewater treatment. The absorption peak of 4-NP shifted from 317 to 400 nm after adding $NaBH_4$, causing a color change from light yellow to yellowish green [Fig. 12]. With the catalyst, the 4-NP peak gradually decreased, and the 4-AP peaks at 232 and 304 nm emerged. After 30 minutes, the 4-NP peak disappeared, indicating complete conversion to 4-AP. Among the tested nanocomposites, CZ/ES showed the highest catalytic activity, likely due to having more surface reaction sites and faster electron transfer channels.[171]

Xin *et al.*[172] used MESM as a sorbent to remove heavy metals from aqueous solutions and produced metal-MESM composites *in situ* using MESM as a template. During adsorption, MESM fibers and metal ions form stable composites through electrostatic interactions and bonding. The reduction in coordinated metal ions on MESM was achieved using $NaBH_4$. The Cu^{2+}

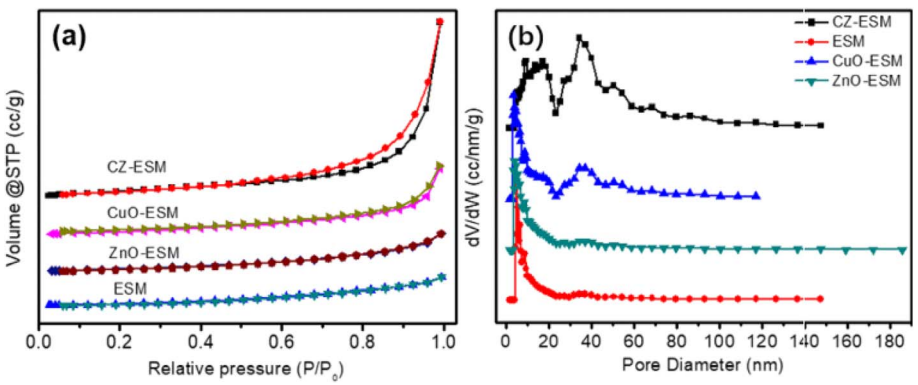

Fig. 11 (a) N_2 adsorption–desorption isotherms and (b) pore size distributions of different nanocomposites. This figure has been adapted/reproduced from ref. 171 with permission from *Chemical Engineering Journal*, copyright 2019.

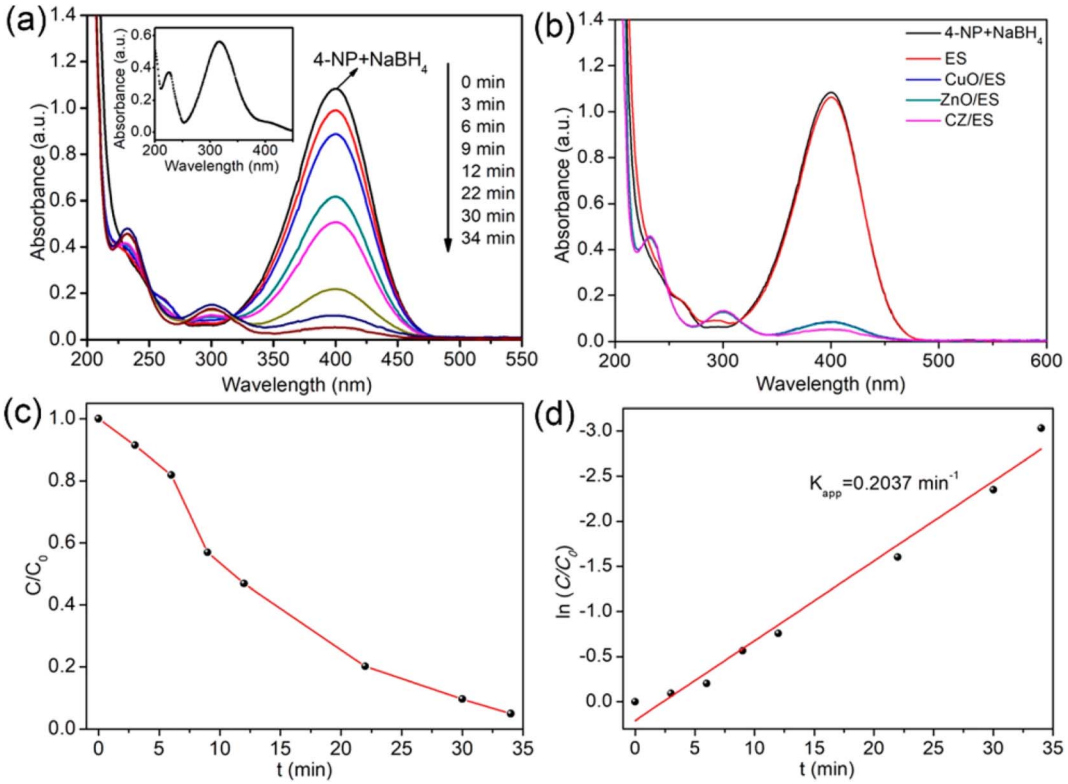

Fig. 12 (a) 4-NP reduction kinetics with ZC-EMS nanocomposites; (b) various catalysts for 4-NP reduction; (c) and (d) plots of C/C_0 and ln C/C_0 *vs.* reaction time. This figure has been adapted/reproduced from ref. 171 with permission from *Chemical Engineering Journal*, copyright 2021.

adsorption capacity of MESM increased with pH, peaking at pH 4.5, whereas the Ag^+ adsorption capacity increased significantly with pH, reaching a maximum at pH 5.5. In a mixed solution, Cu^{2+} adsorption decreased in the presence of Ag^+, whereas Ag^+ adsorption capacity showed a modest reduction. The presence of CuNAPs and AgNAPs on MESM facilitated the catalytic reduction of 4-nitrophenol (4-NP) to 4-aminophenol (4-AP), with the absorbance peak shifting from 400 to 300 nm, indicating successful conversion. MESM alone did not exhibit catalytic activity, serving only as a carrier. The catalytic potential of the metal-MESM composites in the reduction of 4-NP.

4.5.3.2.1 Critical description. Nanotechnology modified matter at the atomic or molecular level: nanoparticles (NAPs) are used in biomedicine, medicine, environmental remediation, and energy generation. Metal nanoparticles like gold and copper can enhance living conditions, making biological synthesis popular. Copper, needed for metabolism, is poisonous at high exposure levels and comes in metallic, ionic, and synthetic CuNAPs. CuNAPs are utilized in greases, polymers, inks, and wastewater treatment due to their antibacterial characteristics; however, their tiny size and acidic ion release make them hazardous. The size, shape, and surface coating of nanoparticles are critical for understanding their toxicological processes. Eggshell-based catalysts improve the environment, as reported in previous research. Methylene blue photodegradation by 97% was achieved using ESM/cuprous oxide biomass catalysts. As peroxymonosulfate activators, CuO/eggshells removed approximately 100% of the reactive blue. The carbamazepine elimination catalytic performance of the CuFeOx/eggshells was also high. Preda *et al.*[158] reported reduced photocatalytic activity in zinc oxide and copper oxide composites containing more copper. Environmentally friendly copper–iron oxide–eggshell nanocomposites were obtained. Tetracycline hydrochloride degradation was achieved by 93% using ESs–CuS composite catalyst. CuO/eggshell nanocomposites converted 4-nitrophenol to 4-aminophenol, whereas the CuO–ZnO version improved sorption and catalysis. MESM composites could be used in environmental applications since they absorb heavy metals and reduce 4-nitrophenol. CuNAPs balance their benefits with health and environmental hazards, and the material structure and synthesis processes are crucial for performance.

4.5.3.3 Antibacterial activity. Phuthotham *et al.*[152] demonstrated the antibacterial activity of eggshell powder by modifying it with in situ-produced CuNPs and Cu_2ONPs using a hydrothermal technique. The eggshell powder, composed of approximately 95% $CaCO_3$ and 5% organic components, was altered to incorporate Cu-based nanoparticles ranging from 50 to 120 nm with an average size of 90 nm. The modification involved the hydrothermal process, where collagen proteins in eggshells react with copper sulfate, reducing Cu^{2+} to Cu^0. While the unmodified eggshell powder showed no antibacterial activity, the modified version created large clearance zones, indicating strong antibacterial properties against both Gram-negative and Gram-positive bacteria [Table 3].

Table 3 Diameters of the zones formed by different samples

Sample	Code	*E. coli* (mm)	*P. aeruginosa* (mm)	*S. aureus* (mm)	*B. licheniformis* (mm)
ESP	O	No clear zone	No clear zone	No clear zone	No clear zone
MESP	Y	38	36	40	38
Cu_2O	A	16	20	161	24
$CuSO_4 \cdot 5H_2O$	B	24	19	17	25

4.5.3.4 Coupling reaction. Kim *et al.*[173] demonstrated that a cuprous oxide/silicon dioxide (SiO_2) eggshell nanocatalyst was effective and stable for producing $C_{15}H_{13}NO$ from C_7H_5ClO and C_8H_6. The TEM images show homogeneous SiO_2 nanospheres with an average diameter of 305 ± 18 nm. Meso-porous SiO_2 shells deposited onto the nanospheres using cetyl trimethyl ammonium bromide resulted in larger m-silica ESs measuring approximately 435 nm, with a 65 nm thick mesoporous SiO_2 shell. Cuprous oxide nanoparticles, 2–3 nm in size and single-crystalline, were well integrated into the SiO_2 mesopores. A lattice spacing of 0.246 nm corresponds to the (111) plane in cubic phase cuprous oxide. The Debye–Scherrer equation estimated the mean particle size as 2 nm. The nanocatalyst's total pore volume was reduced by ∼54% compared to pristine m-silica ESs due to the occupied copper oxide nanoparticles, although both materials had identical pore size distributions in the 2–3 nm range, reflecting the size of the Cu_2O crystallites.

4.5.3.5 Sensing applications. An adaptation of the carbon paste electrode (CEP) for sensitive L-Tyr measurement in human blood samples was created by Kamel *et al.*, who used chitosan gel as a binder. The nanocomposite was constructed from eggshell waste and copper nanoparticles. Using chitosan gel instead of paraffin oil, which is typically used to fabricate CPE, improved electrode sensitivity and selectivity were observed. Using square wave voltammetry, the electrochemical parameters of the oxidation of L-Tyr onto the surface of the created electrode (CuNPs@ESh/CS/CEP) were improved. This helped ensure that the electrode was as effective as possible.[174]

4.6 Passivation of copper nanoclusters

4.6.1 Synthesis of copper nanoclusters *via* eggshells. Eggshell-capped copper nanoclusters offer several advantages, including eco-friendliness, cost-effectiveness, and biocompatibility. The use of eggshells, a natural waste material, as a capping agent aligns with sustainable practices and reduces the need for synthetic stabilizers. These nanoclusters exhibit enhanced stability, preventing aggregation and ensuring uniformity in size, which is crucial for consistent performance in applications such as catalysis and biosensing. Additionally, the biocompatible nature of eggshells makes these nanoclusters suitable for medical and environmental applications, providing a safer and greener alternative to conventional materials.

4.6.2 Applications

4.6.2.1 Eggshell–Cu nanoparticles for sensing. Using $C_4H_{10}O_2S_2$ as the reducing & capping agent, Li *et al.*[175] presented a luminous 2D nanocomposite at room temperature by generating luminescent Cu NACs *in situ* and embedding them in natural monolithic ESM. The photo fluorescence performance, enhanced chemical, thermal, and photo stability, easy tailoring, and flexibility were all displayed by the as-prepared Cu NACs/ESM nanocomposite. The nanocomposites could be used as color-converting layers in light-emitting diodes and as test strips for the colorimetric behaviour of silver ions based on luminescence quenching.

ESM was used as the reaction substrate in the fabrication of a red fluorescent nanocomposite membrane (Cu NACs), as demonstrated by Liang *et al.*[176] In reaction with hydrogen peroxide, the composite membrane exhibits distinct quenching properties. The fluorescence of the quenched composite membrane may be restored by incubation in a solution of glutathione (GSH). The sensor platform allows for the dual colorimetric behaviour of H_2O_2 and GSH. The greatest λ_{ex} of the composite membrane was 344 nm, whereas the λ_{em} of the membrane was 617 nm. The composite membrane did not exhibit a change in emission peak location between 280 and 420 nm, and there was no wavelength dependency. The results also show the optical characteristics of the composite membrane after natural drying. After drying, the composite membrane's λ_{ex} (359 nm) and λ_{em} (601 nm) were changed. The composite membrane did not exhibit a change in emission peak location between 280 and 420 nm, and there was no wavelength dependency. The results also show the optical characteristics of the composite membrane after natural drying. After drying, the composite membrane's λ_{ex} (359 nm) and λ_{em} (601 nm) were changed. The red fluorescent composite membrane's FL remains undeviated in most molecular and ionic solutions, but rose in H_2O_2, and the LOD of H_2O_2 was 73 nM.

4.6.2.2 Eggshell–Cu nanoparticles for dye degradation. Li *et al.*[177] produced orange and red emitting CuNACs embedded in ESM utilizing reducing reagents such as hydrazine hydrate, hydroxylamine hydrochloride, and Vitamin C at ambient temperature. Cu NACs@ESM nano composites had high photo and chemical stability, making them suitable for a variety of applications. XPS research showed the presence of Cu(0) on the ESM, with two significant peaks at 932.2 eV and 952.2 eV, representing Cu $2p_{3/2}$ and Cu $2p_{1/2}$, respectively.[178,179] The absence of a Cu $2p_{3/2}$ satellite peak at 942 eV indicates the absence of copper(II) in the CuNCs@ESM. CuNACs@ESM emitted red fluorescence with a peak at 652 nm and maximal excitation at 370 nm. Cu NACs implanted in monolithic ESM exhibit excitation-independent properties, indicating uniform size and restricted distribution. XPS examination revealed Cu(0) embedded in ESM, with a total copper concentration of 2.4%, as determined by inductively coupled plasma atomic emission

spectroscopy (ICP-AES). After adding monolithic Cu NACs@ESM, the blue hue of the methylene blue solution decreased, and a colorless product, leucomethylene blue (LMB), was formed. The blue color of the Cu NCs@ESM nanocomposite remained almost unchanged when serial ESM controls without CuNACs were added to the MB solutions and incubated for a longer time. The incorporated CuNACs contributed to the observed catalytic performance similar to Cu NACs prepared using wet chemistry methods. The CuNACs@ESM catalyst effectively reduced the absorption peak at 662 nm of the original methylene blue dye in just 2 minutes, eliminating the need for additional reducing agents or UV irradiation.

5 Synergism between copper and eggshell

Synergism occurs when two or more substances interact to produce a combined effect greater than the sum of their individual effects.[180] This concept applies to the combination of copper and eggshells, where the unique properties of each material are enhanced when they form a composite.[181] Copper, known for its catalytic, antimicrobial, and adsorption capabilities, binds effectively with the eggshells, which are primarily composed of calcium carbonate ($CaCO_3$).[4] The eggshells provide a porous surface with a high surface area, offering numerous active sites for copper adhesion. The interaction between copper and carbonate ions in eggshells can occur through ion exchange or complexation processes, forming a stable composite material. Additionally, the organic matrix of eggshells, which includes proteins and other biopolymers, can further facilitate copper binding through coordination bonds. This natural synergy between the eggshell properties and copper's reactive nature results in a composite material with significantly enhanced properties, such as increased adsorption capacity, improved catalytic efficiency, and greater antimicrobial activity.[7] The eggshell acts as a supportive matrix, increasing the surface area for copper to act upon, thereby improving reaction efficiency in catalysis, enhancing the adsorption of heavy metals or pollutants in water treatment, and boosting antimicrobial effectiveness. This synergistic relationship between copper and eggshells makes the composite particularly beneficial for environmental applications, offering a sustainable, cost-effective solution with superior efficiency compared to using either material independently.

5.1 Mechanism of interaction between copper and eggshell

The mechanism between eggshell and copper involves adsorption and ion exchange processes, which are facilitated by the chemical properties of both materials. Here is how it works:

(1) Adsorption: the eggshell, which is composed mostly of calcium carbonate ($CaCO_3$), has a porous structure with a high surface area, which provides numerous active sites for copper ions to adhere to. When copper, in the form of ions or nanoparticles, is introduced to the eggshell, it is adsorbed onto the surface of the eggshell particles. This adsorption was driven by electrostatic interactions between the positively charged copper ions and the negatively charged sites on the eggshell.

(2) Ion exchange: in some cases, there may also be an ion exchange process, where calcium ions (Ca^{2+}) from the eggshell are exchanged with copper ions (Cu^{2+}) from the solution. This exchange can lead to a more stable binding of copper to the eggshell surface, thereby forming a new phase or compound.

(3) Complexation: the organic components of the eggshell, such as proteins and other biopolymers, interact with copper ions through coordination bonds, further stabilizing the copper on the eggshell surface. These interactions enhance the material's overall stability and functionality.

These mechanisms collectively lead to the formation of a copper–eggshell composite in which copper is effectively bound to the eggshell, resulting in improved properties such as increased adsorption capacity, catalytic activity, and antimicrobial effects [Fig. 13]. Moreover, modified eggshells can effectively adsorb Cu^{2+} due to their strong affinity towards copper. Therefore, the synergism between copper and eggshell is an important aspect that requires review in this regard.

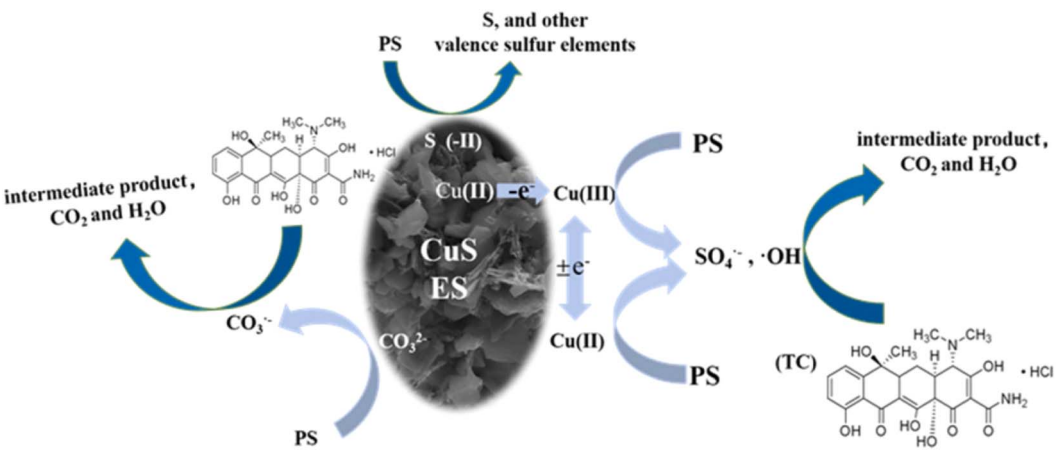

Fig. 13 Mechanism between copper and eggshells. This figure has been adapted/reproduced from ref. 169 with permission from *Molecular Catalysis*, copyright 2021.

6. Eggshells of different birds

Bird eggshells, particularly those from chicken eggs, are most commonly used to synthesize nanoparticles. The widespread availability and low cost of chicken eggs make them popular for research and industrial applications.[11] Chicken eggshells are rich in calcium carbonate ($CaCO_3$), a key component in various nanoparticle synthesis processes. Eggshells can be processed and used as a source of calcium, which is then utilized to create various types of nanoparticles, including calcium oxide (CaO), calcium carbonate ($CaCO_3$) nanoparticles, and others.

From duck eggshells, calcium oxide (CaO) nanoparticles have been effectively manufactured using the ball milling process, followed by simple calcination at a temperature of 700 degrees Celsius for seven hours. A clear relationship was observed between milling time and average eggshell powder diameter. The average diameter of eggshell powder decreased with longer milling time. The impact of milling balls on the top surface of eggshell particles reduces their diameter.[182]

$CaCO_3$ nanopowder derived from uncooked quail eggshells, as well as analyses of the nanostructure and particle size, chemical composition, organics (C/H/N) components, and practical groups, to provide endorsements for the utilization of this form of nanoparticles.[183] Quail egg yolk, which has a high amount of both vitamins and proteins, was produced for the green synthesis reaction and then employed to produce platinum nanoparticles in the reaction medium, as proven by Nadaroglu *et al.*[184] Pt nanoparticles that were produced from quail egg yolk medium were cubic and ranged in size from 7 to 50 nanometers. Nadaroglu *et al.*[185] used quail egg yolks, which have high protein and vitamin content, for the green synthesis of gold NPs. Au NPs were observed at 20–50 nm in quail egg yolk medium.

Copper nanoparticles were synthesized only from chicken egg (hen's egg). There is no report available for the synthesis of copper nanoparticles using duck and quail nanoparticles. The synthesis of copper nanoparticles using hen eggs may be attributed to the specific properties and composition of hen eggs that make them suitable for this process. Hen eggs contain a well-characterized and consistent protein composition, particularly egg white (albumen) and yolk, which are crucial in acting as reducing and stabilizing agents during nanoparticle formation. The proteins in hen eggs, such as ovalbumin, might be more effective in reducing copper ions to nanoparticles and stabilizing the particles to prevent aggregation. Additionally, hen eggs are larger and more widely available than quail and duck eggs, providing abundant and easily accessible material for research. This availability, coupled with the established use of hen eggs in the scientific literature, makes them a convenient and reliable choice for nanoparticle synthesis. Furthermore, the chemical environment of hen eggs, including factors like pH and ion content, might create a more favorable setting for the efficient synthesis of copper nanoparticles. While quail and duck eggs can be used for similar purposes, they might require different conditions or might not be as effective. Therefore, this research has predominantly focused on using hen eggs.

7. Circular economy

Using eggshell-derived copper nanoparticles in a circular economy for environmental benefits is an innovative approach that leverages waste materials and nanotechnology to create sustainable solutions. The concept revolves around transforming waste eggshells, a common byproduct of the food industry, into valuable copper nanoparticles that can be utilized in various applications, thereby contributing to waste reduction, resource efficiency, and environmental protection. Eggshells are primarily composed of calcium carbonate, which can be processed and used as a precursor material in the synthesis of copper nanoparticles. The process begins with the collection and cleaning of waste eggshells. The shells are then calcined at high temperatures to remove organic impurities and convert calcium carbonate into calcium oxide. The calcium oxide can then be reacted with a copper precursor, such as copper sulfate, under controlled conditions to produce copper nanoparticles.

The produced copper nanoparticles have a wide range of applications, particularly in environmental remediation and agriculture. For example, they can be used as catalysts in chemical reactions to degrade pollutants in wastewater, thereby contributing to cleaner water resources. Additionally, in agriculture, these nanoparticles can be employed as antifungal agents or fertilizers, enhancing crop growth and reducing the need for chemical pesticides and fertilizers, which often have harmful environmental impacts. By incorporating eggshell-derived copper nanoparticles into a circular economy framework, this approach helps to close the loop on waste, turning a potential environmental burden (eggshell waste) into a valuable resource. This not only reduces the amount of waste sent to landfills but also decreases the need for virgin materials, conserving natural resources and reducing the carbon footprint associated with mining and processing raw materials. Many metal nanoparticles have been reported with the passivation of eggshells. Many metals are toxic. However, some non-hazardous metals are also available in the literature (*e.g.*, Fe, Zn)[186] with eggshell passivation. Copper nanoparticles have been well studied for the circular economy. Ravi *et al.*[187] reported a circular economy involving waste printing circuit boards and copper oxide nanoparticles. Benguigui *et al.*[188] analyzed the considerable therapeutic properties in medical science. Additionally, proper capping helps copper nanoparticles with efficient drug-loading property and cell viability.[189]

On this ground, animal waste eggshells (non-expensive) are a potential candidate for the circular economy.

Moreover, the circular economy model promotes sustainable production and consumption patterns by encouraging the reuse, recycling, and upcycling of materials. The integration of eggshell-derived copper nanoparticles aligns with this model by ensuring that waste materials are reintegrated into the production cycle, creating a closed-loop system that minimizes environmental impact.

8. Conclusions and future perspectives

Eggshell-capped nanoparticles have shown significant potential for copper ion adsorption due to their high surface area and the presence of functional groups that effectively interact with copper ions. Eggshells, a readily available waste by-product, not only offer an eco-friendly and cost-effective approach but also provide a natural porous structure that enhances the adsorption capacity of the nanoparticles. These nanoparticles are capable of adsorbing large amounts of copper ions, making them suitable for water purification applications, with the added advantage of being reusable without significant loss of efficiency over multiple cycles. Eggshell-capped copper nanoparticles have demonstrated excellent catalytic activity, antimicrobial properties, and potential for various environmental applications. The eggshell matrix stabilizes the copper nanoparticles, improving their stability, activity, and preventing agglomeration, thus maintaining their high surface area and reactivity. These nanoparticles can be used in chemical reactions, pollutant degradation, and antimicrobial agents, offering a biocompatible and environmentally friendly alternative to traditional methods. The integration of eggshells into nanoparticle synthesis not only aligns with green chemistry principles but also results in products that are sustainable, less toxic, and more practical for real-world applications in catalysis, environmental remediation, and biomedicine.

Copper can react with eggshells because eggshells are primarily composed of calcium carbonate ($CaCO_3$). When copper encounters calcium carbonate, a chemical reaction can occur, especially in the presence of acids or acidic conditions. In an acidic environment, calcium carbonate in eggshell reacts with acid to form calcium ions, carbon dioxide gas, and water. Copper is a relatively reactive metal that can sometimes be involved in reactions in which acids are present, leading to the dissolution or alteration of the eggshell's surface. In the absence of acidic conditions, the reaction between copper and eggshell is minimal because copper is less reactive with the neutral or slightly acidic substances found in eggshell. Egg yolk does not react with copper because it primarily consists of proteins and fats, which do not have strong reactions with copper under normal conditions. Copper is more likely to react with acidic substances, and egg yolk is generally neutral to slightly acidic. In addition, the proteins in the yolk can form a protective layer that prevents direct contact between copper and any reactive components. This shows the synergistic behavior between eggshell and copper [Fig. 14].

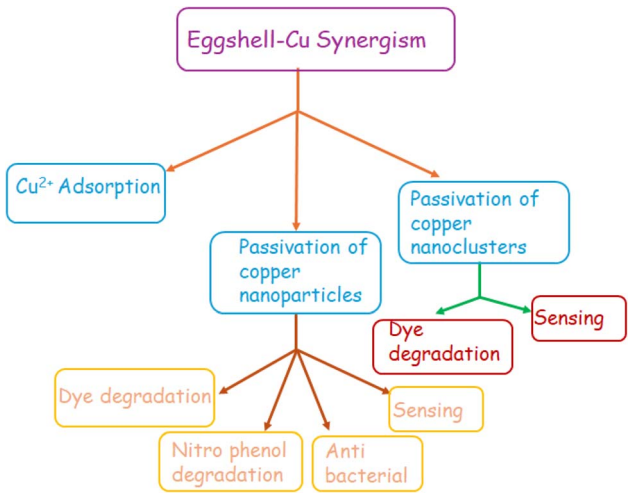

Fig. 14 Synergistic behaviour of eggshell–Cu for myriad applications.

This paper presents a cocktail of synergism and circular economy for a myriad of applications. It may be an asset to be a young scientist venturing into the field of environmental nanotechnology and material science.

A review was available on transforming eggshells into useful products was reported by Waheed *et al.*[190] Chong *et al.*[191] reviewed the features of eggshells in powder form. Samiullah *et al.*[192] reviewed the color of eggshells in brown hen eggs. However, there are no review articles available on the involvement of eggshells in synthesizing and capping nanoparticles/nanoclusters with applications. Recently, a lot of publications have been available on the nanometric applications of eggshells. Thus, we strongly perceive the importance of this review for the related young scientists.

Consent to participate

All the participants have checked the paper and have consented to the submission.

Consent to publish

All the participants consented to publish.

Data availability

No primary research results, software or code has been included and no new data were generated or analysed as part of this review.

Author contributions

Priyanka Sharma reviewed the literature and wrote a major part of the manuscript. Mainak Ganguly, the corresponding author, designed and checked the manuscript. Ankita Doi reviewed and wrote some parts of the manuscript.

Conflicts of interest

There is no competing interest to disclose.

References

1 G. Kulshreshtha, L. D'Alba, I. C. Dunn, S. Rehault-Godbert, A. B. Rodriguez-Navarro and M. T. Hincke, Properties, Genetics and Innate Immune Function of the Cuticle in Egg-Laying Species, *Front. Immunol.*, 2022, **13**, 838525.

2 A. Mottet and G. Tempio, Global Poultry Production: Current State and Future Outlook and Challenges, *World's Poult. Sci. J.*, 2017, **73**, 245–256.
3 X. Cuticle, Deposition Duration in the Uterus is Correlated With Eggshell Cuticle Quality in White Leghorn Laying Hens, *Sci. Rep.*, 2021, **11**, 1–12.
4 A. Laca, A. Laca and M. Díaz, Eggshell waste as catalyst: A review, *J. Environ. Manage.*, 2017, **15**, 351–359.
5 S. Park, K. S. Choi, D. Lee, D. Kim, K. T. Lim, K.-H. Lee, H. Seonwoo and J. Kim, Eggshell membrane: Review and impact on engineering, *Biosyst. Eng.*, 2016, **151**, 446–463.
6 H. M. Hamada, B. A. Tayeh, A. Al-Attar, F. M. Yahaya, K. Muthusamy and A. M. Humada, The present state of the use of eggshell powder in concrete: A review, *J. Build. Eng.*, 2020, **32**, 101583.
7 H. Faridi and A. Arabhosseini, Application of eggshell wastes as valuable and utilizable products: A review, *Res. Agric. Eng.*, 2018, **64**, 104–114.
8 M. M. Bain, Recent advances in the assessment of eggshell quality and their future application, *World's Poult. Sci. J.*, 2019, **61**, 268–277.
9 I. K. Della-Flora and C. J. de Andrade, Biosynthesis of metallic nanoparticles by bacterial cell-free extract, *Nanoscale*, 2023, **15**, 13886–13908.
10 I. Khan, K. Saeed and I. Khan, Nanoparticles: Properties, applications and toxicities, *Arabian J. Chem.*, 2019, **12**, 908–931.
11 M. Vert, Y. Doi, K.-H. Hellwich, M. Hess, P. Hodge, P. Kubisa, M. Rinaudo and F. Schué, Terminology for biorelated polymers and applications (IUPAC Recommendations 2012), *Pure Appl. Chem.*, 2012, **84**, 377–410.
12 A. Cayuela, M. L. Soriano, C. Carrillo-Carrion and M. Valcarcel, Semiconductor and carbon based fluorescent nanodots: the need for consistency, *Chem. Commun.*, 2016, **52**, 1311–1326.
13 I. Diez and R. H. Ras, Fluorescent silver nanoclusters, *Nanoscale*, 2011, **3**, 1963–70.
14 M. Chandler, O. Mhevchenko, J. L. Vivero-Escoto, C. D. Striplin and K. A. Afonin, *DNA Templated Synth. Educ.*, 2020, **97**, 1992–1996.
15 J. Yu, From Coinage Metal to Luminescent Nanodots: The Impact of Size on Silver's Optical Properties, *J. Chem. Educ.*, 2014, **91**, 701–704.
16 T. M. Ayers, S. T. Akin, C. J. Dibble and M. A. Duncan, Laser Desorption Time-of-Flight Mass Spectrometry of Inorganic Nanoclusters: An Experiment for Physical Chemistry or Advanced Instrumentation Laboratories, *J. Chem. Educ.*, 2014, **91**, 291–296.
17 S. Dehnen, A. Eichhöfer and D. Fenske, *Eur. J. Inorg. Chem.*, 2002, **2002**, 279.
18 Q. Zhu, X. Huang, Y. Zeng, K. Sun, L. Zhou, Y. Liu, L. Luo, S. Tian and X. Sun, Controllable synthesis and electrocatalytic applications of atomically precise gold nanoclusters, *Nanoscale Adv.*, 2021, **3**, 6330–6341.
19 O. Fuhr, S. Dehnen and D. Fenske, *Chem. Soc. Rev.*, 2013, **42**, 1871–1906.
20 C. Coughlan, M. Ibáñez, O. Dobrozhan, A. Singh, A. Cabot and K. M. Ryan, *Chem. Rev.*, 2017, **117**, 5865–6109.
21 W. W. Lu and W. Chen, *Chin. Sci. Bull.*, 2012, **57**, 41–47.
22 N. K. Das and S. Mukherjee, *Phys. Sci. Rev.*, 2018, **3**, 1–22.
23 S. Sharma, K. K. Chakrahari, J.-Y. Saillard and C. W. Liu, *Acc. Chem. Res.*, 2018, **51**, 2475–2483.
24 A. Baghdasaryan and T. Bürgi, Copper nanoclusters: designed synthesis, structural diversity, and multiplatform, *Nanoscale*, 2021, **13**, 6283–6340.
25 F. Wu, M. Misra and A. K. Mohanty, Challenges and new opportunities on barrier performance of biodegradable polymers for sustainable packaging, *Prog. Polym. Sci.*, 2021, **117**, 101395.
26 A. Riley, C. J. Sturrock, S. J. Mooney and M. R. Luck, Quantification of Eggshell Microstructure Using X-Ray Micro Computed Tomography, *Br. Poult. Sci.*, 2014, **55**, 311–320.
27 G. Kulshreshtha, A. Rodriguez-Navarro, E. Sanchez-Rodriguez, T. Diep and M. T. Hincke, Cuticle and Pore Plug Properties in the Table Egg, *Poultry Sci.*, 2018, **97**, 1382–1390.
28 M. Ladouce, T. Barakat, B.-L. Su, O. Deparis and S. R. Mouchet, Scattering of Ultraviolet Light by Avian Eggshells, *Faraday Discuss.*, 2020, **223**, 63–80.
29 P. C. M. Simons, in *Ultrastructure of the Hen Eggshell and its Physiological Interpretation*, Centre for Agricultural Publishing and Documentation, Wageningen, 1971, vol. 1.
30 R. G. Board, Properties of Avian Egg Shells and Their Adaptive Value, *Biol. Rev.*, 1982, **57**, 1–28.
31 R. Burley and D. Vadehra, The Egg Shell and Shell Membrane: Properties and Synthesis, in *The Avian Egg Chemistry and Biology*, John Wiley & Sons, Inc., New York, 1989, pp. 25–64.
32 A. Rodriguez-Navarro, O. Kalin, Y. Nys and J. M. Garcia-Ruiz, Influence of the Microstructure on the Shell Strength of Eggs Laid by Hens of Different Ages, *Br. Poult. Sci.*, 2002, **43**, 395–403.
33 O. Wellman-Labadie, J. Picman and M. T. Hincke, Antimicrobial Activity of Cuticle and Outer Eggshell Protein Extracts From Three Species of Domestic Birds, *Br. Poult. Sci.*, 2008, **49**, 133–143.
34 M. Rose-Martel and M. T. Hincke, Protein Constituents of the Eggshell: Eggshell-Specific Matrix Proteins, *Cell. Mol. Life Sci.*, 2009, **66**, 2707–2719.
35 S. Kusuda, A. Swasawa, O. Doi, Y. Ohya and N. Yoshizaki, Diversity of the Cuticle Layer of Avian Eggshells, *J. Poultry Sci.*, 2011, **48**, 119–124.
36 K. Palka, Chemical and functional properties of food components, in *Chemical and Functional Properties of Food Components*, ed. Z. E. Sikorski, CRC Press, Boca Raton, 3rd edn, 2006, pp. 15–28.
37 T. Nakano, N. I. Ikawa and L. Ozimek, Chemical composition of chicken eggshell and shell membranes, *Poult. Sci.*, 2003, **82**, 510–514.
38 Y. Nys, J. Gautron, J. M. Garcia-Ruiz and M. T. Hincke, Avian eggshell mineralization: biochemical and functional

characterization of matrix proteins, *C. R. Palevol*, 2004, **3**, 549–562.

39 M. L. H. Rose and M. T. Hincke, Protein constituents of the eggshell: eggshell-specific matrix proteins, *Cell. Mol. Life Sci.*, 2009, **66**, 2707–2719.

40 Y. S. Ok, J. E. Yang, Y. S. Zhang, S. J. Kim and D. Y. Chung, Heavy metal adsorption by a formulated zeolitePortland cement mixture, *J. Hazard. Mater.*, 2007, **147**, 91–96.

41 D. S. R. Krishna, A. Siddharthan, S. Seshadri and T. S. Kumar, A novel route for synthesis of nanocrystalline hydroxyapatite from eggshell waste, *J. Mater. Sci.: Mater. Med.*, 2007, **18**, 1735–1743.

42 X. Zhao, Y. Zhai, Y. Zhou, Z. Liu, Z. Kang, B. Wang, M. D. Regulacio and D.-P. Yang, Transforming oyster shell and rice husk biowaste into functional calcium silicate board with highly-efficient photo-enhanced antimicrobial activities, *Constr. Build. Mater.*, 2024, **411**, 134505.

43 W. J. Stadelman and O. Cotterill, *Egg Science and Technology*, CRC Press, Boca Raton, FL, USA, 4th edn, 1995, ISBN 9781560228554.

44 S. E. Solomon, The eggshell: Strength, structure and function, *Br. Poult. Sci.*, 2010, **51**, 52–59.

45 K. A. Altammar, A review on nanoparticles: characteristics, synthesis, applications, and challenges, *Front. Microbiol.*, 2023, **14**, 1155622.

46 R. Javed, M. Zia, S. Naz, S. O. Aisida, N. ul Ain and Q. Ao, Role of capping agents in the application of nanoparticles in biomedicine and environmental remediation: recent trends and future prospects, *J. Nanobiotechnol.*, 2020, **18**, 172.

47 A. Mittal, M. Teotia, R. K. Soni and J. Mittal, Applications of egg shell and egg shell membrane as adsorbents: A review, *J. Mol. Liq.*, 2016, **223**, 376–387.

48 M. Baláž, E. V Boldyreva, D. Rybin, S. Pavlović, D. Rodríguez-Padrón, T. Mudrinić and R. Luque, State-of-the-Art of Eggshell Waste in Materials Science: Recent Advances in Catalysis, Pharmaceutical Applications, and Mechanochemistry, *Front. Bioeng. Biotechnol.*, 2021, **27**, 612567.

49 L. Iftikhar, I. Ahmad, M. Saleem, A. Rasheed and A. Waseem, Exploring the chemistry of waste eggshells and its diverse applications, *Waste Manage.*, 2024, **189**, 348–363.

50 T. S. Sampath Kumar, K. Madhumathi and R. Jayasree, Eggshell Waste: A Gold Mine for Sustainable Bioceramics, *J. Indian Inst. Sci.*, 2022, **102**, 599–620.

51 S. Owuamanam and D. Cree, Progress of Bio-Calcium Carbonate Waste Eggshell and Seashell Fillers in Polymer Composites: A Review, *J. Comput. Sci.*, 2020, **2**, 70.

52 P. Rosaiah, D. Yue, K. Dayanidhi, K. Ramachandran, P. Vadivel, N. Sheik Eusuff, V. R. M. Reddy and W. K. Kim, Eggshells & Eggshell Membranes – A Sustainable Resource for energy storage and energy conversion applications: A critical review, *Adv. Colloid Interface Sci.*, 2024, **327**, 103144.

53 H. Badamasi, S. O. Sanni, O. T. Ore, A. A. Bayode, D. T. Koko, O. K. Akeremale and S. S. Emmanuel, Eggshell waste materials-supported metal oxide nanocomposites for the efficient photocatalytic degradation of organic dyes in water and wastewater: A review, *Bioresour. Technol. Rep.*, 2024, **26**, 101865.

54 Y. Nys and J. Gautron, Structure and formation of the eggshell, in *Bioactive Egg Compounds*, ed. R. Huopalati, R. Lopez-Fandino, M. Anton and R. Schade, Springer-Verlag, Berlin Heidelberg (Germany), 2007, p. 99e102.

55 E. C. Y. Li-Chang and H. O. Kim, Structure and chemical composition of eggs, in *Egg Bioscience and Biotechnology*, ed. Y. Mine, John Wiley & Sons Inc., USA, 2008, p. 1e96.

56 A. B. A. Mohammed, M. A. Al-Saman and A. A. Tayel, Antibacterialactivityoffusionfrombiosynthesized acidocin/silvernanoparticlesanditsapplication foreggshelldecontamination, *J. Basic Microbiol.*, 2017, **3**, 1–8.

57 M. E. E. Zin, P. Moolkaew, T. Junyusen and W. Sutapun, Preparationofhybridparticles ofAgnanoparticlesand eggshell calciumcarbonate andtheirantimicrobial efficiencyagainstbeef extractedbacteria, *R. Soc. Open Sci.*, 2023, **10**, 221197.

58 M. Liang, R. Su, R. Huang, W. Qi, Y. Yu, L. Wang and Z. He, Facile *in Situ* Synthesis of Silver Nanoparticles on Procyanidin-Grafted Eggshell Membrane and Their Catalytic Properties, *ACS Appl. Mater. Interfaces*, 2014, **6**, 4638–4649.

59 M. Ayub, M. Bashir, F. Majid, R. Shahid, B. S. Khan, A. Saeed, M. R. Shaik, M. K. Baji Shaik and M. Khan, Eggshell-Mediated Hematite Nanoparticles: Synthesis and Their Biomedical, Mineralization, and Biodegradation Applications, *Crystals*, 2023, **13**, 1699.

60 S. Datta, B. Kanjilal and P. Sarkar, Silver nanoparticles decorated eggshell membrane as an effective platform for interference free sensing of dopamine, *J. Environ. Sci. Health, Part A: Toxic/Hazard. Subst. Environ. Eng.*, 2018, **53**, 1048–1055.

61 Y. Nys, M. T. Hincke, J. L. Arias, J. M. Garcia-Ruiz and S. Solomon, Avian Eggshell Mineralization, *Avian Poultry Biol. Rev.*, 1999, **10**, 143–166.

62 Y. J. Nys, J. M. Gautron and M. . T. Garcia-Ruiz, Hincke, Avian eggshell mineralization: biochemical and functional characterization of matrix proteins, *C. R. Palevol*, 2004, **3**, 549–562.

63 M. T Hincke, Y. Nys, J. Gautron, K. Mann, A. B. Rodriguez-Navarro and M. D McKee, The eggshell: structure, composition and mineralization, *Front. Biosci.*, 2012, **4**, 1266–1280.

64 (*a*) A. Laca, A. Laca and M. Díaz, Eggshell waste as catalyst: A review, *J. Environ. Manag.*, 2017, **197**, 351–359; (*b*) U. Akbar, S. Srivastava, A. Hussain Dar, S. A. Mondol, V. K. Pandey, T. Majeeda and U. S. Sidiqia, Potential of cold plasma in enhancing egg white protein for sustainable food applications: a comprehensive review, *Sustainable Food Technol.*, 2024, **2**, 1631.

65 M. Baláž, E. V Boldyreva, D. Rybin, S. Pavlović, D. Rodríguez-Padrón, T. Mudrinić and R. Luque, State-of-the-Art of Eggshell Waste in Materials Science: Recent Advances in Catalysis, Pharmaceutical Applications, and Mechanochemistry, *Front. Bioeng. Biotechnol.*, 2021, **8**, 612567.

66 E. Mosaddegh, Ultrasonic-assisted preparation of nano eggshell powder: A novel catalyst in green and highly efficient synthesis of 2-aminochromenes, *Ultrason. Sonochem.*, 2013, **20**, 1436–1441.

67 K. Yorseng, S. Siengchin, B. Ashok and A. V. Rajulu, Nanocomposite egg shell powder with *in situ* generated silver nanoparticles using inherent collagen as reducing agent, *J. Bioresour. Bioprod.*, 2020, **5**, 101–107.

68 B. W. Chong, R. Othman, P. J. Ramadhansyah, S. I. Doh and X. Li, Properties of concrete with eggshell powder: A review, *Phys. Chem. Earth*, 2020, **120**, 102951.

69 T. Al Seadi and J. B. Holm-Nielsen III, 2 Agricultural wastes, *Waste Manage. Ser.*, 2004, **4**, 207–215.

70 T. A. E. Ahmed, L. Wu, M. Younes and M. Hincke, Biotechnological Applications of Eggshell: Recent Advances, *Front. Bioeng. Biotechnol.*, 2021, **6**, 675364.

71 C. M. Cordeiro and M. T. Hincke, Recent patents on eggshell: shell and membrane applications, *Recent Pat. Food Nutr. Agric.*, 2011, **3**, 1–8.

72 M. Martin-Luengo, M. Yates, M. Ramos, E. Saez Rojo, A. Martinez Serrano, L. Gonzalez Gil and E. R. Hitzky, biomaterials from beer manufacture waste for bone growth scaffolds, *Green Chem. Lett. Rev.*, 2011, **4**, 229–233.

73 N. Verma, V. Kumar and M. C. Bansal, Utilization of egg shell waste in cellulase production by Neurospora crassa under Wheat bran-based solid state fermentation, *Pol. J. Environ. Stud.*, 2012, **21**, 491–497.

74 L. Dupoirieux, D. Pourquier and F. Souyris, Powdered eggshell: a pilot study on a new bone substitute for use in maxillofacial surgery, *J. Cranio-Maxillofacial Surg.*, 1995, **23**, 187–194.

75 C. Balázsi, F. Wéber, Z. Kövér, E. Horváth and C. Németh, Preparation of calcium–phosphate bioceramics from natural resources, *J. Eur. Ceram. Soc.*, 2007, **27**, 1601–1606.

76 W. T. Tsai, K. J. Hsien, H. C. Hsu, C. M. Lin, K. Y. Lin and C. H. Chiu, Utilization of ground eggshell waste as an adsorbent for the removal of dyes from aqueous solution, *Bioresour. Technol.*, 2008, **99**, 1623–1629.

77 P. Ducheyne, W. Van Raemdonck, J. Heughebaert and M. Heughebaert, Structural analysis of hydroxyapatite coatings on titanium, *Biomaterials*, 1986, **7**, 97–103.

78 G. Gergely, F. Wéber, I. Lukács, A. L. Tóth, Z. E. Horváth, J. Mihály and C. Balázsi, Preparation and characterization of hydroxyapatite from eggshell, *Ceram. Int.*, 2010, **36**, 803–806.

79 E. M. Rivera, M. Araiza, W. Brostow, V. M. Castano, J. DiazEstrada, R. Hernandez and J. R. Rodriguez, Synthesis of hydroxyapatite from eggshells, *Mater. Lett.*, 1999, **41**, 128–134.

80 R. Bal, B. Tope, T. Das, S. Hegde and S. Sivasanker, Alkaliloaded silica, a solid base: investigation by FTIR spectroscopy of adsorbed CO2 and its catalytic activity, *J. Catal.*, 2001, **204**, 358–363.

81 O. N. Syazwani, U. Rashid and Y. H. T. Yap, Low-cost solid catalyst derived from waste Cyrtopleura costata (Angel Wing Shell) for biodiesel production using microalgae oil, *Energy Convers. Manag.*, 2015, **101**, 749–756.

82 N. Nakatani, H. Takamori, K. Takeda and H. Sakugawa, Transesterification of soybean oil using combusted oyster shell waste as a catalyst, *Bioresour. Technol.*, 2009, **100**, 1510–1513.

83 V. L. Gole and P. R. Gogate, A review on intensification of synthesis of biodiesel from sustainable feed stock using sonochemical reactors, *Chem. Eng. Process.*, 2012, **53**, 1–9.

84 R. Rezaei, M. Mohadesi and G. Moradi, Optimization of biodiesel production using waste mussel shell catalyst, *Fuel*, 2013, **109**, 534–541.

85 M. R. R. Hamester, P. S. Balzer and D. Becker, Characterization of calcium carbonate obtained from oyster and mussel shells and incorporation in polypropylene, *Mater. Res.*, 2012, **15**, 204–208.

86 D. Oliveira, P. Benelli and E. Amante, A literature review on adding value to solid residues: egg shells, *J. Cleaner Prod.*, 2013, **46**, 42–47.

87 H. J. Park, S. W. Jeong, J. K. Yang, B. G. Kim and S. M. Lee, Removal of heavy metals using waste eggshell, *J. Environ. Sci.*, 2007, **19**, 1436–1441.

88 O. A. Habeeb, F. M. Yasin and U. A. Danhassan, Characterization and application of chicken eggshell as green adsorbents for removal of H2 S from wastewaters, *IOSR J. Environ. Sci., Toxicol. Food Technol.*, 2014, **8**, 7–12.

89 M. Baláž, J. Ficeriová and J. Briančin, Influence of milling on the adsorption ability of eggshell waste, *Chemosphere*, 2016, **146**, 458–471.

90 H. Faridi and A. Arabhosseini, Application of eggshell wastes as valuable and utilizable products: A review, *Res. Agric. Eng.*, 2018, **64**, 104–114.

91 D. Athanasiadou, W. Jiang, D. Goldbaum, A. Saleem, K. Basu, M. C. Pacella, C. F. Bohm, R. C. Chromik, M. T. Hincke, A. B. Rodriquez-Navarro, H. Vali, S. E. Wolf, J. J. Gray, K. H. Bui and M. D. McKee, Nanostructure, ostepontin, and mechanical properties of calcitic avian eggshell, *Sci. Adv.*, 2018, **4**, 1–13.

92 C. Rodriguez-Navarro, E. Ruiz-Agudo, A. Luque, A. B. Rodriguez-Navarro and M. O. Huertas, Thermal decomposition of calcite: Mechanisms of formation and textural evolution of CaO nanocrystals, *Am. Mineral.*, 2009, **94**, 578–593.

93 F. S. Murakami, P. O. Rodrigues, C. M. T. de Campos and M. A. S. Silva, Physicochemical study of CaCO3 from egg shells, *Food Sci. Technol.*, 2007, **27**, 658–682.

94 M. S. Tizo, L. A. V. Blanco, A. C. Q. Cagas, B. R. B. Dela Cruz, J. C. Encoy, J. V. Gunting, R. O. Arazo and V. I. F. Mabayo, Efficiency of calcium carbonate from eggshells as an adsorbent for cadmium removal in aqueous solution, *Sustainable Environ. Res.*, 2018, **28**, 326–332.

95 M. Minakshi, S. Higley, C. Baur, D. R. G. Mitchell, R. T. Jones and M. Fichtner, Calcined chicken eggshell

electrode for battery and supercapacitor applications, *RSC Adv.*, 2019, **9**, 26981–26995.

96 M. Y. Chou, T. A. Lee, Y. S. Lin, S. Y. Hsu, M. F. Wang, P. H. Li, P. H. Huang, W. C. Lu and J. H. Ho, On the removal efficiency of copper ions in wastewater using calcined waste eggshells as natural adsorbents, *Sci. Rep.*, 2020, **13**, 437.

97 S. S. Hosseini, A. Hamadi, R. Foroutan, S. J. Peighambardoust and B. Ramavandi, Decontamination of Cd2+ and Pb2+ from aqueous solution using a magnetic nanocomposite of eggshell/starch/Fe3O4, *J. Water Process Eng.*, 2022, **48**, 102911.

98 N. Y. Mezenner and A. Bensmaili, Kinetics and thermodynamic study of phosphate adsorption on iron hydroxide-eggshell waste, *Chem. Eng. J.*, 2009, **147**, 87–96.

99 E.-S. R. E. Hassan, M. Rostom, F. E. Farghaly and M. A. Abdel Khalek, Bio-sorption for tannery effluent treatment using eggshell wastes; kinetics, isotherm and thermodynamic study, *Egypt. J. Pet.*, 2020, **29**, 273–278.

100 A. Rahmani-Sani, P. Singh, P. Raizada, E. C. Lima, I. Anastopoulos, D. A. Giannakoudakis, S. Sivamani, T. A. Dontsova and A. Hosseini-Bandegharaei, Use of chicken feather and eggshell to synthesize a novel magnetized activated carbon for sorption of heavy metal ions, *Bioresour. Technol.*, 2020, **297**, 122452.

101 L. G. Djemmoe, T. E. Njanja, M. C. Ngaha Deussi and K. I. Tonle, Assessment of copper(II) biosorption from aqueous solution by agricultural and industrial residues, *C. R. Chim.*, 2016, **19**, 841–849.

102 W. Su, Y. Yang, H. Dai and L. Jiang, Biosorption of heavy metal ions from aqueous solution of Chinese fir bark modified by sodium hypochlorite, *Bioresources*, 2015, **10**, 6993–7008.

103 A. Imessaoudene, S. Cheikh, J. C. Bollinger, L. Belkhiri, A. Tiri, A. Bouzaza, A. El Jery, A. Assadi, A. Amrane and L. Mouni, Zeolite waste characterization and use as low-cost, ecofriendly, and sustainable material for malachite green and methylene blue dyes removal: Box-behnken design, kinetics, and thermodynamics, *Appl. Sci.*, 2022, **12**, 7587.

104 M. Marković, M. Gorgievski, N. Štrbac, V. Grekulović, K. Božinović, M. Zdravković and M. Vuković, Raw Eggshell as an Adsorbent for Copper Ions Biosorption—Equilibrium, Kinetic, Thermodynamic and Process Optimization Studies, *Metals*, 2023, **13**, 206.

105 W. Zheng, X. M. Li, Q. Yang, G. M. Zeng, X. X. Shen, Y. Zhang and J. J. Liu, Adsorption of Cd (II) and Cu (II) from aqueous solution by carbonate hydroxylapatite derived from eggshell waste, *J. Hazard. Mater.*, 2007, **147**, 534–539.

106 I. S. Okure, P. C. Okafor and U. J. Ibok, Adsorption of Cu2+, As3+, and Cd2+ ions from aqueous solution by eggshell, *Global J. Pure Appl. Sci.*, 2010, **16**, 407–416.

107 M. Horsfall Jr and A. I. Spiff, Effects of temperature on the sorption of Pb2+ and Cd2+ from aqueous solution by Caladium bicolor (Wild Cocoyam) biomass, *Electron. J. Biotechnol.*, 2005, **8**, 43–50.

108 E. A. Ofudje, E. F. Sodiya, F. H. Ibadin, A. A. Ogundiran, S. O. Alayande and O. A. Osideko, Mechanism of Cu2+ and reactive yellow 145 dye adsorption onto eggshell waste as low-cost adsorbent, *Chem. Ecol.*, 2021, **37**, 268–289.

109 O. J. D. L. Redlich and D. L. Peterson, A useful adsorption isotherm, *J. Phys. Chem.*, 1959, **63**, 1024.

110 R. Sips, Combined form of Langmuir and Freundlich equations, *J. Chem. Phys.*, 1948, **16**, 490–495.

111 E. A. Ofudje, O. D. Williams and K. K. Asogwa, Assessment of Langmuir, Freundlich, and Rubunin-Radushhkevich adsorption isotherms in the study of the biosorption of Mn (II) ions from aqueous solution by untreated and acid-treated corn shaft, *Int. J. Sci. Eng. Res.*, 2013, **4**, 1628–1634.

112 A. I. Adeogun, E. A. Ofudje and M. A. Idowu, Equilibrium, kinetic, and thermodynamic studies of the biosorption of Mn (II) ions from aqueous solute and acid-treated corncob, *Bioresources*, 2011, **6**, 4117–4134.

113 M. Ganguly and P. A. Ariya, Novel Technology for the Removal of Brilliant Green from Water: Influence of Post-Oxidation, Environmental Conditions, and Capping, *ACS Omega*, 2019, **4**, 12107–12120.

114 E. A. Ofudje, A. I. Adeogun and M. A. Idowu, Simultaneous removals of cadmium (II) ions and reactive yellow 4 dye from aqueous solution by bone meal derived apatite: kinetics, equilibrium, and thermodynamic evaluations, *J. Anal. Sci. Technol.*, 2020, **11**, 7.

115 M. Bashir, S. Tyagi and A. P. Annachhatre, Adsorption of copper from aqueous solution onto agricultural adsorbents: kinetics and isotherm studies, *Mater. Today: Proc.*, 2020, **28**, 1833–1840.

116 S. Yasin, S. Hami, M. S. A. Eltoum, A. S. Hame and M. A. Almaleeh, A Unique Modified Eggshell Method as a Model to Reduce and Remove Copper (II) from Aqueous Solutions for Water Treatment, *Orient. J. Chem.*, 2023, **39**, 694–702.

117 J. H. Chen and Y. H. Huang, Efficient adsorption of copper ion from aqueous solution by amino-functioned porous eggshell membrane, *Desalin. Water Treat.*, 2016, **57**, 12178–12191.

118 M. Arami, N. Y. Limaee and N. M. Mahmoodi, Investigation on the adsorption capability of egg shell membrane towards model textile dyes, *Chemosphere*, 2006, **65**, 1999–2008.

119 M. Kalbarczyk, A. Szcześ and D. Sternik, The preparation of calcium phosphate adsorbent from natural calcium resource and its application for copper ion removal, *Environ. Sci. Pollut. Res.*, 2021, **28**, 1725–1733.

120 D. Núñez, J. A. Serrano, A. Mancisidor, E. Elgueta, K. Varaprasad, P. Oyarzun, R. Caceres, W. Ide and B. L. Rivas, Heavy metal removal from aqueous systems using hydroxyapatite nanocrystals derived from clam shells, *RSC Adv.*, 2019, **9**, 22883–22890.

121 A. Ansari, S. Vahedi, O. Tavakoli, M. Khoobi and M. A. Faramarzi, Novel Fe3O4/hydroxyapatite/β-cyclodextrin nanocomposite adsorbent: synthesis and

application in heavy metal removal from aqueous solution, *Appl. Organomet. Chem.*, 2019, **33**, 4634.

122 M. A. Orlova, A. L. Nikolaev, T. P. Trofimova, A. V. Severin, A. V. Gopin, N. S. Zolotova, V. K. Dolgova and A. P. Orlov, Specific properties of hydroxyapatite as a potential transporter of copper ions and its complexes, *Russ. Chem. Bull.*, 2019, **68**, 1102–1108.

123 J. Mohammadnezhad, F. Khodabakhshi-Soreshjani and H. Bakhshi, Preparation and evaluation of chitosan-coated eggshell particles as copper (II) biosorbent, *Desalin. Water Treat.*, 2016, **57**, 1693–1704.

124 M. Ahmad, A. R. A. Usman, S. S. Lee, S.-C. Kim, J.-H. Joo, J. E. Yang and Y. S. Ok, Eggshell and coral wastes as low cost sorbents for the removal of Pb2+, Cd2+ and Cu2+ from aqueous solutions, *J. Ind. Eng. Chem.*, 2012, **18**, 198–204.

125 H. A. Aziz, M. N. Adlan and K. S. Ariffin, Heavy metals (Cd, Pb, Zn, Ni, Cu and Cr(III)) removal from water in Malaysia: Post treatment by high quality limestone, *Bioresour. Technol.*, 2008, **99**, 1578–1583.

126 M. J. Madiabu, J. Untung, I. Solihat and A. M. Ichzan, Equilibrium and Kinetic Study of Removal Copper (II) from Aqueous Solution Using Chicken Eggshells: Low-Cost Sorbent, *Molekul*, 2021, **16**, 28–37.

127 L. Cao, Z. W. Kang, Q. Ding, X. Zhang, H. Lin, M. Lin and D. P. Yang, Rapid pyrolysis of Cu2+-polluted eggshell membrane into a functional Cu2+-Cu+/biochar for ultrasensitive electrochemical detection of nitrite in water, *Sci. Total Environ.*, 2020, **723**, 138008.

128 O. Ayodele, S. J. Olusegun, O. O. Oluwasina, E. A. Okoronkwo, E. O. Olanipekun, N. D. Mohallem, W. G. Guimarães, B. L. D. M. Gomes, G. D. O. Souza and H. A. Duarte, Experimental and theoretical studies of the adsorption of Cu and Ni ions from wastewater by hydroxyapatite derived from eggshells, *Environ. Nanotechnol., Monit. Manage.*, 2021, **15**, 100439.

129 D. N. Thanh, P. Novak, J. Vejpravova, H. N. Vu, J. Lederer and T. Munshi, Removal of copper and nickel from water using nanocomposite of magnetic hydroxyapatite nanorods, *J. Magn. Magn. Mater.*, 2018, **456**, 451–460.

130 S. Zamani, E. Salahi and I. Mobasherpour, Removal of nickel from aqueous solution by nano-hydroxyapatite originated from Persian Gulf Corals, *Can. Chem. Trans.*, 2013, **1**, 173–190.

131 F. M. Kasperiski, E. C. Lima, C. S. Umpierres, S. Glaydson, P. Silas, D. Ramos, S. L. P. Dias, C. Saucier and B. Janaina, Production of porous activated carbons from Caesalpinia ferrea seed pod wastes: highly efficient removal of captopril from aqueous solutions, *J. Cleaner Prod.*, 2018, **197**, 919–929.

132 R. Attinti, D. Sarkar, K. R. Barrett and R. Datta, Adsorption of arsenic(V) from aqueous solutions by goethite/silica nanocomposite, *Int. J. Environ. Sci. Technol.*, 2015, **12**, 3905–3914.

133 Z. Wei, C. Xu and B. Li, Application of waste eggshell as low-cost solid catalyst for biodiesel production, *Bioresour. Technol.*, 2009, **100**, 2883–2885.

134 J. Goli and O. Sahu, Development of heterogeneous alkali catalyst from waste chicken eggshell for biodiesel production, *Renewable Energy*, 2018, **128**, 142–154.

135 D. A. Oliveira, P. Benelli and E. R. Amante, A literature review on adding value to solid residues: egg shells, *J. Cleaner Prod.*, 2013, **46**, 42–47.

136 Y. Han, J. Trakulmututa, T. Amornsakchai, S. Boonyuen., N. Prigyai and S. M. Smith, Eggshell-Derived Copper Calcium Hydroxy Double Salts and Their Activity for Treatment of Highly Polluted Wastewater, *ACS Omega*, 2023, **8**, 46663–46675.

137 J. Trakulmututa, K. Uraisin, S. Pornsuwan and S. M. Smith, Effects of acetate and nitrate ions on radical and intercalation reactions initiated by CuZn hydroxy double salts, *Mater. Res. Bull.*, 2023, **162**, 112181.

138 T. Kameda, T. Yamazaki and T. Yoshioka, Preparation and characterization of Mg-Al layered double hydroxides intercalated with benzenesulfonate and benzenedisulfonate, *Microporous Mesoporous Mater.*, 2008, **114**, 410–415.

139 B. D. Harishchandra, M. Pappuswamy, P. U. Antony, G. Shama, A. Pragatheesh, V. A. Arumugam, T. Periyaswamy and R. Sundaram, Copper nanoparticles: a review on synthesis, characterization and applications, *Asian Pac. J. Cancer Biol.*, 2020, **5**, 201–210.

140 P. Sharma, M. Ganguly and A. Doi, Complexation–reduction method for the evolution of nanoparticles to detect Ag^{+} and Cu^{2+}: a synergistic approach, *Appl. Nanosci.*, 2024, **14**, 739–751.

141 P. Sharma, M. Ganguly, A. Doi and M. Sahu, Recent advances in the application of copper nanocluster and copper nanoparticle in water for heavy metals detection: A review, *Environ. Nanotechnol., Monit. Manage.*, 2024, **22**, 100970.

142 P. Sharma and M. Ganguly, Copper-enhanced fluorescence: a novel platform for the sensing of hydrogen peroxide, *New J. Chem.*, 2023, **47**, 7481–7485.

143 J. Pal, M. Ganguly, C. Mondal, A. Roy, Y. Negishi and T. Pal, Crystal-Plane-Dependent Etching of Cuprous Oxide Nanoparticles of Varied Shapes and Their Application in Visible Light Photocatalysis, *J. Phys. Chem. C*, 2013, **117**, 24640–24653.

144 M. Ganguly, A. Pal, Y. Negishi and T. Pal, Diiminic Schiff Bases: An Intriguing Class of Compounds for a Copper-Nanoparticle-Induced Fluorescence Study, *Chem. Eur.*, 2012, **18**, 15845–15855.

145 Y. Zhang, C. Xue, Y. Zhang, Q. Zhang, K. Zhang, Y. Liu, Z. Shan, W. Qiu, G. Chen, N. Li, H. Zhang, J. Zhao and D.-P. Yang, Cocktail effect of ionic patch driven by triboelectric nanogenerator for diabetic wound healing, *Chin. Chem. Lett.*, 2024, **35**, 109196.

146 M. Ganguly, J. Pal, C. Mondal, A. Pal and T. Pal, Intriguing Manipulation of Metal-Enhanced Fluorescence for the Detection of CuII and Cysteine, *Chem. Eur.*, 2014, **20**, 12470–12476.

147 P. Sharma, M. Ganguly and A. Doi, Analytical developments in the synergism of copper particles and cysteine: a review, *Nanoscale Adv.*, 2024, **6**, 3476–3493.

148 M. C. Crisan, M. Teodora and M. Lucian, Copper Nanoparticles: Synthesis and Characterization, Physiology, Toxicity and Antimicrobial Applications, *Appl. Sci.*, 2022, **12**, 141.

149 R. Lu, W. Hao, L. Kong, K. Zhao, H. Bai and Z. Liu, A simple method for the synthesis of copper nanoparticles from metastable intermediates, *RSC Adv.*, 2023, **13**, 14361–14369.

150 M. J. Woźniak-Budych, K. Staszak and M. Staszak, Copper and Copper-Based Nanoparticles in Medicine—Perspectives and Challenges, *Molecules*, 2023, **28**, 6687.

151 T. Ameh and C. M. Sayes, The potential exposure and hazards of copper nanoparticles: A review, *Environ. Toxicol. Pharmacol.*, 2019, **71**, 103220.

152 M. Phuthotham, S. Siengchin, B. Ashok and A. Varada Rajulu, Modification of egg shell powder with *in situ* generated copper and cuprous oxide nanoparticles by hydrothermal method, *Mater. Res. Express*, 2020, **7**, 015010.

153 T. Wu, J. Cao and X. Jiang, In situ synthesis of oxygen-deficient Cu_2O on eggshell membranes and study of its efficient photocatalytic activity, *Appl. Surf. Sci.*, 2023, **612**, 155752.

154 J. Xu, S. Hu, L. Min and S. Wang, Waste eggshell-supported CuO used as heterogeneous catalyst for reactive blue 19 degradation through peroxymonosulfate activation (CuO/eggshell catalysts activate PMS to degrade reactive blue 19), *Water Sci. Technol.*, 2022, **11**, 3271–3284.

155 A. Rastogi, S. R. Al-Abed and D. D. Dionysiou, Sulfate radical-based ferrous–peroxymonosulfate oxidative system for PCBs degradation in aqueous and sediment systems, *Appl. Catal., B*, 2009, **85**, 171–179.

156 Y. Pang, L. Kong, D. Chen, G. Yuvaraja and S. Mehmood, Facilely synthesized cobalt doped hydroxyapatite as hydroxyl promoted peroxymonosulfate activator for degradation of Rhodamine B, *J. Hazard. Mater.*, 2020, **384**, 121447.

157 Y. Gao, Z. Zhao, L. Song, D. Cao, S. Zhou, T. Gao, J. Shang and X. Cheng, Eggshell supported Cu doped FeO_x magnetic nanoparticles as peroxymonosulfate activator for carbamazepine degradation, *Chem. Eng. J.*, 2023, **454**, 140282.

158 N. Preda, A. Costas, M. Enculescu and I. Enculescu, Biomorphic 3D fibrous networks based on ZnO, CuO and ZnO–CuO composite nanostructures prepared from eggshell membranes, *Mater. Chem. Phys.*, 2020, **240**, 122205.

159 M. Ahmad and J. Zhu, ZnO based advanced functional nanostructures: synthesis, properties and applications, *J. Mater. Chem.*, 2011, **21**, 599–614.

160 A. S. Zoolfakar, R. A. Rani, A. J. Morfa, A. P. O'Mullane and K. Kalantar-Zadeh, Nanostructured copper oxide semiconductors: a perspective on materials, synthesis methods and applications, *J. Mater. Chem. C*, 2014, **2**, 5247–5270.

161 J. Fang and Y. Xuan, Investigation of optical absorption and photothermal conversion characteristics of binary CuO/ZnO nanofluids, *RSC Adv.*, 2017, **7**, 56023–56033.

162 D. Malwal and P. Gopinath, Enhanced photocatalytic activity of hierarchical three dimensional metal oxide@CuO nanostructures towards the degradation of Congo red dye under solar radiation, *Catal. Sci. Technol.*, 2016, **6**, 4458–4472.

163 A. Naseri, M. Samadi, N. M. Mahmoodi, A. Pourjavadi, H. Mehdipour and A. Z. Moshfegh, Tuning composition of electrospun ZnO/CuO nanofibers: toward controllable and efficient solar photocatalytic degradation of organic pollutants, *J. Phys. Chem. C*, 2017, **121**, 3327–3338.

164 M. Nasrollahzadeh, S. M. Sajadi and A. Hatamifard, Waste chicken eggshell as a natural valuable resource and environmentally benign support for biosynthesis of catalytically active Cu/eggshell, Fe_3O_4/eggshell and Cu/Fe_3O_4/eggshell nanocomposite, *Appl. Catal., B*, 2016, **191**, 209–227.

165 H. Jacquemyn, R. Brys, O. Honnay and M. J. Hutchings, *J. Evol.*, 2009, **97**, 360–377.

166 N. Aziz, M. Hassan Mehmood, H. Salman Siddiqi, S.-U. Rehman Mandukhail, F. Sadiq, W. Maan and A. Hassan Gilani, *Hypertens. Res.*, 2009, **32**, 997–1003.

167 L. Dormont, R. Delle-Vedove, J.-M. Bessière and B. Schatz, *Phytochemistry*, 2014, **100**, 51–59.

168 S. V. Bhat, B. A. Nagasampagi and M. Sivakumar, *Chemistry of Natural Products*, Narosa Publishing House, New Delhi, 2005, pp. 585–683.

169 X. Gao, Y. Chen, Z. Kang, B. Wang, L. Sun, D.-P. Yang and W. Du, Enhanced degradation of aqueous tetracycline hydrochloride by integrating eggshell-derived CaCO3/CuS nanocomposite with advanced oxidation process, *Mol. Catal.*, 2021, **501**, 111380.

170 S. M. Sajadi, K. Kolo, S. M. Abdullah, S. M. Hamad, H. S. Khalid and A. T. Yassein, Green synthesis of highly recyclable CuO/eggshell nanocomposite to efficient removal of aromatic containing compounds and reduction of 4-Nitrophenol at room temperature, *Surf. Interfaces*, 2018, **13**, 205–215.

171 X. He, D.-P. Yang, X. Zhang, M. Liu, Z. Kang, C. Lin, N. Jia and R. Luque, Waste eggshell membrane-templated CuO-ZnO nanocomposites with enhanced adsorption, catalysis and antibacterial properties for water purification, *Chem. Eng. J.*, 2019, **369**, 621–633.

172 Y. Xin, C. Li, J. Liu, J. Liu, Y. Liu, W. He and Y. Gao, Adsorption of heavy metal with modified eggshell membrane and the *in situ* synthesis of Cu –Ag/modified eggshell membrane composites, *R. Soc. Open Sci.*, 2018, **5**, 180532.

173 S. Kim, S. W. Kang, A. Kim, M. Yusuf, J. C. Park and K. H. Park, A highly efficient nano-sized Cu2O/SiO2 egg-shell catalyst for C–C coupling reactions, *RSC Adv.*, 2018, **8**, 6200–6205.

174 R. M. Kamel, F. A. M. Abdel-aal, F. A. Mohamed, A. Asmaa, M. O. Abdel-Malek, A. A. Othman and I. M. Abdel-Maaboud, Copper @ eggshell nanocomposite/chitosan gelified carbon paste electrode as an electrochemical biosensor for l-tyrosine analysis as a biomarker in the serum of

normal and liver disease patients, *Microchem. J.*, 2024, **201**, 110703.

175 C. Li, C. Shao, L. Li, a X. Liu and M. Liu, *In situ* fabrication of a luminescent copper nanocluster/eggshell membrane composite and its application in visual detection of Ag^+ ions, light-emitting diodes and surface patterning, *Photochem. Photobiol. Sci.*, 2019, **18**, 2942–2951.

176 M. Liang, L. Yuan, C. Shao, X. Zheng, Q. Song, Z. Gu and S. Lu, Sequential Visual Sensing of H2O2 and GSH Based on Fluorescent Copper Nanoclusters Incorporated Eggshell Membrane, *IEEE Sens. J.*, 2023, **23**, 18142–18149.

177 L. Li, M. Huang, X. Liu, D. Sun and C. Shao, In Situ Generation of Fluorescent Copper Nanoclusters Embedded in Monolithic Eggshell Membrane: Properties and Applications, *Materials*, 2018, **11**, 1913.

178 W. T. Wei, Y. Z. Lu, W. Chen and S. W. Chen, One-Pot synthesis, photoluminescence, and electrocatalytic properties of subnanometer-sized copper clusters, *J. Am. Chem. Soc.*, 2011, **133**, 2060–2063.

179 N. Goswami, A. Giri, M. S. Bootharaju, P. L. Xavier, T. Pradeep and S. K. Pal, Copper quantum clusters in protein matrix: Potential sensor of Pb^{2+} ion, *Anal. Chem.*, 2011, **83**, 9676–9680.

180 M. Ganguly, J. Jana, A. Pal and T. Pal, Synergism of gold and silver invites enhanced fluorescence for practical applications, *RSC Adv.*, 2016, **6**, 17683–17703.

181 K. W. Shinato, F.-F. Huang, Y.-P. Xue, L. Wen, Y. Jin, Y.-J. Mao and Y. Luo, Synergistic inhibitive effect of cysteine and iodide ions on corrosion behavior of copper in acidic sulfate solution, *Rare Met.*, 2020, **40**, 1317–1328.

182 A. Y. Nuryantini, C. D. Dewi Sundari and B. Halimahtussa'diah, Wahid Nuryadin Synthesis and Characterization of Calcium Oxide Nanoparticles from Duck Eggshells using Ball Milling Methods, *J. Kim. Valensi*, 2019, **5**, 231–235.

183 N. S. Ahmed, F. H. Kamil, A. Ali Hasso, A. Nazar Abduljawaad, T. F. Saleh and S. K. Mahmood, Calcium carbonate nanoparticles of quail's egg shells: Synthesis and characterizations, *J. Mech. Behav. Mater.*, 2022, **31**, 1–7.

184 H. Nadaroglu, A. A. Gungor, S. Ince and A. Babagil, Green synthesis and characterisation of platinum nanoparticles using quail egg yolk, *Spectrochim. Acta*, 2017, **172**, 43–47.

185 H. Nadaroglu, S. Ince and A. Alayli Gungor, Green synthesis of gold nanoparticles using quail egg yolk and investigation of potential application areas, *Green Process. Synth.*, 2017, **6**, 43–48.

186 M. C. Tucker, D. Lambelet, M. Oueslati, B. Williams, W.-C. J. Wang and A. Weber, Improved low-cost, non-hazardous, all-iron cell for the developing world, *J. Power Sources*, 2016, **332**, 111–117.

187 B. Ravi, A. Duraisamy and T. Marimuthu, A novel integrated circular economy approach in green synthesis of copper oxide nanoparticles from waste printed circuit boards and utilization of its residue for preparation of carbon engulfed nano polymer membrane, *J. Cleaner Prod.*, 2022, **383**, 135457.

188 M. Benguigui, i. S. Weitz, M. timaner, t. Kan, D. Shechter, O. perlman, S. Sivan, Z. Raviv, H. Azhari and Y. Shaked, copper oxide nanoparticles inhibit pancreatic tumor growth primarily by targeting tumor in itiating cells, *Sci. Rep.*, 2019, **1**, 12613.

189 S. A. Ahmed, M. H. Gaber, A. A. Salama and S. A. Ali, Efficacy of copper nanoparticles encapsulated in soya lecithin liposomes in treating breast cancer cells (MCF-7) in vitro, *Sci. Rep.*, 2023, **13**, 15576.

190 M. Waheed, M. Yousaf, A. Shehzad, M. Inam-Ur-Raheem, M. K. I. Khan, M. R. Khan, N. Ahmad and A. R. M. Aadil, Channelling eggshell waste to valuable and utilizable products: A comprehensive review, *Trends Food Sci. Technol.*, 2020, **106**, 78–90.

191 B. W. Chong, R. Othman, P. J. Ramadhansyah, S. I. Doh and X. Li, Properties of concrete with eggshell powder: A review, *Phys. Chem. Earth, Parts A/B/C*, 2020, **120**, 102951.

192 S. Samiullah, J. R. Roberts and K. Chousalkar, Eggshell color in brown-egg laying hens - a review, *Poult. Sci.*, 2015, **10**, 2566–2575.